

1 **'Co-evolution' of Uranium Concentration and Oxygen Stable Isotope in**
2 **Phosphate Rocks**

3 Y.Sun^{1,2*}, W. Amelung^{1,2}, B. Wu¹, S. Haneklaus³, M. Maekawa³, A. Lücke¹, E. Schnug³,
4 R. Bol¹

5 ¹Institute of Bio- and Geosciences: Agrosphere (IBG-3), Forschungszentrum Jülich
6 GmbH, 52425 Jülich, Germany

7 ²University of Bonn, Institute of Crop Science and Resource Conservation, Soil
8 Science and Soil Ecology, Nussallee 13, 53115 Bonn, Germany.

9 ³ Institute for Crop and Soil Science, Julius Kühn-Institut, Federal Research Institute
10 for Cultivated Plants, Bundesallee 69, 38640 Braunschweig, Germany

11

12 * Corresponding author (yajie.sun@uni-bonn.de)

13

14 **Abstract**

15 Phosphate rocks (PRs) used in fertilizer production contain uranium (U), which enters
16 agricultural soils through phosphorus fertilization. However, our knowledge is still
17 limited and cannot explain the different levels of U contamination found in agricultural
18 systems. The paper reviewed the spatial and temporal U variations in PRs to obtain a
19 comprehensive overview of U levels in various PRs worldwide and to investigate why
20 U concentrations in igneous PRs are significantly lower compared to sedimentary PRs,
21 and why less U is present in old sedimentary PRs (Precambrian-Cambrian) than in
22 younger PRs (Ordovician-Neogene). In addition, the natural oxygen isotope
23 compositions of phosphate ($\delta^{18}\text{O}_\text{p}$) in various PRs were determined to identify their
24 origins in relation to their U concentration. The $\delta^{18}\text{O}_\text{p}$ values differed among igneous
25 PRs, old sedimentary PRs, and younger sedimentary PRs. Generally, the PRs with
26 low $\delta^{18}\text{O}_\text{p}$ values had low U concentrations. In igneous PRs, low U concentrations

27 were due to the lack of secondary U enrichment processes after rock formation, with
28 low $\delta^{18}\text{O}_\text{p}$ values resulting from limited isotope fractionation at high temperature.
29 Conversely, in sedimentary PRs, both U concentrations and $\delta^{18}\text{O}_\text{p}$ values were
30 influenced by paleoclimate and paleogeographic features. Overall, there is a time-
31 dependent coincidence of processes altering U concentration and $\delta^{18}\text{O}_\text{p}$ signatures of
32 sedimentary PRs in a similar direction.

33

34 **Highlights**

- 35 • The U contents of phosphate rocks (PRs) increased in the order igneous PRs,
36 old sedimentary PRs (Precambrian-Cambrian), younger sedimentary PRs
37 (Ordovician-Neogene).
- 38 • The values of $\delta^{18}\text{O}_\text{p}$ of PRs increase as follows: igneous PRs, old sedimentary
39 PRs (Precambrian-Cambrian), younger sedimentary PRs (Ordovician-
40 Neogene).
- 41 • In sedimentary PRs, there is a time-dependent coincidence of processes
42 altering U concentration and $\delta^{18}\text{O}_\text{p}$ signatures in a similar direction.

43

44 **Keywords:** phosphate rocks; $\delta^{18}\text{O}_\text{p}$; uranium; $\text{U}/\text{P}_2\text{O}_5$

45

46 **1. Introduction**

47 Phosphorus (P) is a vital nutrient and energy carrier for life and it is thus also an
48 indispensable fertilizer in agriculture including animal husbandry. The main route for
49 the P supply relies on the exploitation of geological phosphate deposits, the availability
50 of which is likely limited to the next 40 to 400 years (Obersteiner et al., 2013). However,
51 phosphate rocks (PRs) also contain a significant amount of uranium (U) (0.3 to 247 mg
52 U kg⁻¹), with typical average concentrations of 75 to 120 mg kg⁻¹ (Altschuler, 1980).

53 Most recently Windmann (2019) reported an average geometric mean in 128
54 sedimentary phosphate rock of 56.9 mg U kg⁻¹, compared to only 7.56 mg U kg⁻¹ in 22
55 rocks of igneous origin. Therefore, mineral P fertilizers produced by PRs may also
56 contain various amount of U which can be added to agricultural soils through the
57 application of mineral P fertilizers (Schnug and Haneklaus, 2015). Depending on the
58 source and the amounts of mineral P fertilizers applied, different levels of U
59 accumulation have been observed in agricultural soils in various countries (e.g.
60 Rothbaum et al., 1979; Bigalke et al., 2018).

61 To avoid potential U contamination and explain the different levels of U accumulation
62 in agricultural soil, it is necessary to reveal the variations of U concentrations in PRs
63 from different deposits. Furthermore, geochemical signatures of PRs are needed to
64 identify the origins of PRs. How and why U concentrations are related to the origin of
65 PRs are the key questions to be understood. Previous studies revealed that, at present,
66 no single element concentration can be used to differentiate PR deposits (Sattouf et
67 al., 2007). An alternative way is to identify the origin of deposits of PRs by using stable
68 isotopes, such as strontium (Sr) isotopes (Sattouf, 2007). For instance, Sattouf et al.
69 (2007) used ⁸⁷Sr/⁸⁶Sr isotope ratios to classify PRs into four different groups: 1)
70 igneous rock phosphates from Russia (Kola), sedimentary rock from: 2) Algeria, Israel,
71 Morocco, Tunisia and Syria, 3) the USA, and 4) Senegal and Togo. In addition,
72 ²³⁴U/²³⁸U ratios can be used to distinguish PRs and P fertilizers originating from the
73 USA and those of other regions (Sattouf et al., 2008).

74 Taking advantage of stable isotope discrimination processes to identify the origin of
75 PRs does not apply for P, because this element does not have different stable isotopes.
76 However, we may take advantage of natural oxygen (O) isotope compositions of
77 phosphate ($\delta^{18}\text{O}_\text{p}$) in the PRs. $\delta^{18}\text{O}_\text{p}$ is selected as a potential indicator of the origin of
78 the phosphate due to the fact that O stable isotope signatures may provide unique

79 information on the paleo-environmental conditions during PRs formation. Based on
80 pioneering research by Longinelli and Nuti (1973), who constructed an empirical
81 equation between inorganic P-water oxygen isotope fractionations and temperature,

$$T = 111.4 - 4.3 (\delta^{18}\text{O}_p - \delta^{18}\text{O}_w)$$

82 where T is the average environmental temperature, $\delta^{18}\text{O}_p$ is the natural oxygen isotope
83 composition of phosphate and $\delta^{18}\text{O}_w$ is that of water. Oxygen in phosphate is bound
84 tightly to P such that isotope exchange of O between phosphate and surrounding water
85 is essentially negligible by abiotic processes even over geological time scales at low
86 temperatures which relevant to earth surface environments (Jaisi and Blake, 2014;
87 Longinelli and Nuti, 1973; Lecuyer et al., 1999; Blake et al., 2010; Shemesh et al.,
88 1983). This is true even at extreme pH values (10 M nitric acid and 14 M NH₄OH) and
89 at high temperature condition(70 °C), which has been proved on laboratory time scales
90 (Blake et al., 2010). However, using the $\delta^{18}\text{O}_p$ value as a tracer for different PR deposits
91 in relation to the occurrence of U is still pending. We therefore aimed to look for
92 possible indicators that can relate the origin of PRs to their U and P content.

93 This study was performed to contribute to a better background understanding why
94 agricultural soils may show different levels of U contamination through P fertilization.
95 The first part of the paper provides an overview of the spatial and temporal distributions
96 of U in PRs, the second investigates the degree to which the $\delta^{18}\text{O}_p$ values of PRs can
97 reflect their deposition, and the third presents the correlation between the U
98 concentration and the natural $\delta^{18}\text{O}_p$ for different PR deposits. Details on U
99 geochemistry in PRs and other related isotope studies are not re-reviewed here, since
100 this has already been undertaken by several authors, e.g. Jarvis (1995), or Kolodny
101 and Luz (1992).

103

104 **2. Materials and Methods**

105 Data collection

106 Published U concentrations from overall 18 igneous and 277 sedimentary deposits
107 were retrieved from the literatures. To supplement this data, we collected 74
108 sedimentary PRs from 11 countries: Algeria, Brazil, China, Israel, Morocco, Russia,
109 Senegal, South Africa, Syria, Togo, USA, and 9 igneous PRs from Brazil, China, South
110 Africa and Russia. All these PRs samples were analyzed for total U concentration and
111 oxygen isotope composition in phosphate ($\delta^{18}\text{O}_\text{p}$).

112 Uranium analyses

113 Total concentrations of U in PRs were analyzed by inductively coupled plasma
114 spectrometry (ICP-MS, Thermo Fisher Scientific, Bremen, Germany) after the
115 digestion of 0.05 g soil with 0.25 g lithium meta/tetraborate at 1050 °C for 3 h. The
116 analytical error for total concentration measurement by ICP-MS was within 2%.

117 $\delta^{18}\text{O}_\text{p}$ analyses

118 One gram of each ground phosphate rock samples was shaken with 50 ml 1M HCl for
119 16 hours. The soil-acid mixture was then centrifuged for 15 minutes at 1300 g and
120 filtered through Whatman GF/F filters. The supernatant was then used for phosphate
121 purification. The purification procedures followed Tamburini et al. (2010). This method
122 is based on the preparation of ammonium phosphomolybdate salts (APM), which are
123 precipitated by adding ammonium nitrate solution and ammonium molybdate to the
124 sample solution. Subsequently, the APM was dissolved again in citric acid solution and
125 Mg added to produce a magnesium ammonium phosphate mineral precipitate (MAP).
126 The precipitation products were then dissolved with 0.5 mol l⁻¹ nitric acid and purified
127 via a DOWEX® 50 WX8 (200 -400 mesh) cation resin. By adding Ag nitrate solution,

128 the phosphates to be analyzed were precipitated as silver phosphate (Ag_3PO_4). The
129 $\delta^{18}\text{O}_{\text{P}}$ values were finally determined by high temperature reduction of Ag_3PO_4 to CO
130 by a high-temperature conversion isotope ratio mass spectrometry (HTC-IRMS)
131 system, composed of a high temperature oven (HEKA tech GmbH, Germany) and the
132 IRMS Isoprime (Elementar Analysensysteme GmbH, Germany). All measurements
133 were performed together with four in house laboratory Ag_3PO_4 standards spanning as
134 $\delta^{18}\text{O}$ range between 2.2‰ and 33.7‰ Vienna Standard Mean Ocean Water (VSMOW).
135 In house standards were calibrated against two International Atomic Energy Agency
136 (IAEA) benzoic acid standards, IAEA 601 ($\delta^{18}\text{O} = 23.1\text{\textperthousand}$ VSMOW) and IAEA 602
137 ($\delta^{18}\text{O} = 71.3\text{\textperthousand}$ VSMOW). All measured $\delta^{18}\text{O}_{\text{P}}$ values are reported normalized to the
138 VSMOW scale. Analytical uncertainty calculated on replicate analysis of in house
139 standards was better than $\pm 0.25\text{\textperthousand}$.
140 Details of U concentration and oxygen isotope signatures of the different PRs can be
141 found in the supplementary material S1-3.

142

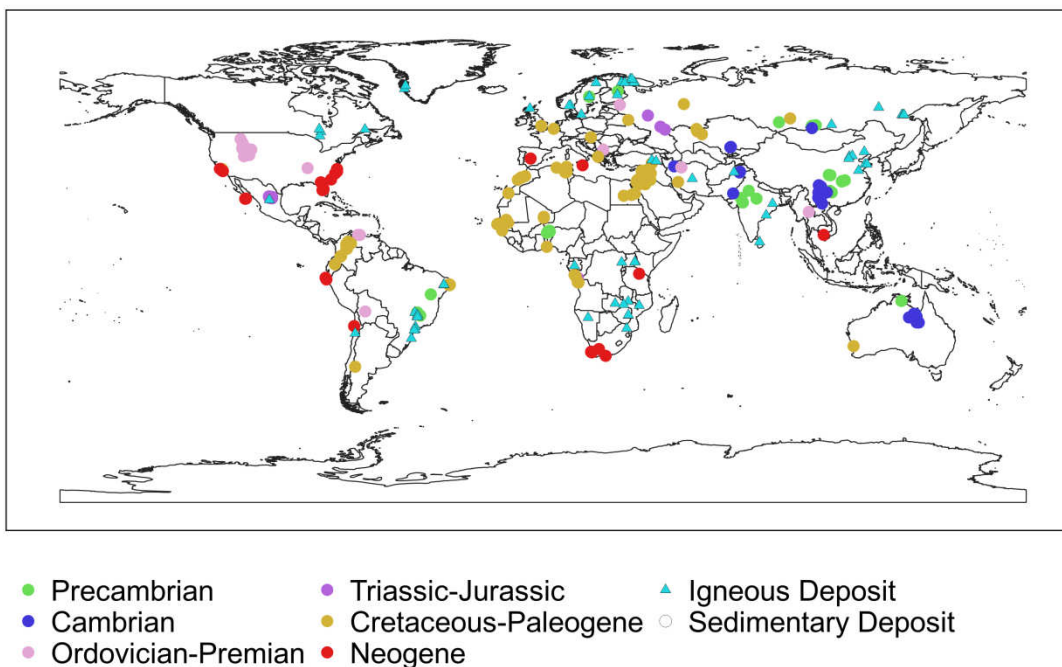
143 **3. Results and Discussion**

144 **3.1 Spatial and temporal distributions of uranium concentrations in phosphate 145 rocks**

146 **3.1.1 Spatial distribution**

147 The main phosphate ores types include marine sediments, igneous rocks and guano.
148 About 75% of the world's phosphate resources are obtained from sedimentary PRs,
149 whereas 15-20% are obtained from igneous deposits (Pufahl and Groat, 2016; Petr,
150 2016). Guano, i.e., mainly deposits from birds, penguins, cormorants and bats, is
151 enriched in P but is not available in sufficient quantities for global use (Pufahl and Groat,
152 2016). The majority of sedimentary phosphate deposits have been formed under

153 marine conditions (e.g. Nathan, 2012) and are quantitatively the most important source
154 of the world's phosphate rocks for fertilizer production (U.S. Geological Survey, 2018).
155 Sedimentary phosphate deposits are found on almost every continent, in North Africa
156 and the Middle East, China, and the United States and range in age from Precambrian
157 to Recent (e.g. Cook, 1984) (Fig. 1). The largest P reserves are found in the Late
158 Cretaceous-Eocene South Tethyan phosphogenic province, hosting 85% of the world's
159 PR reservoir (Cook, 1984).

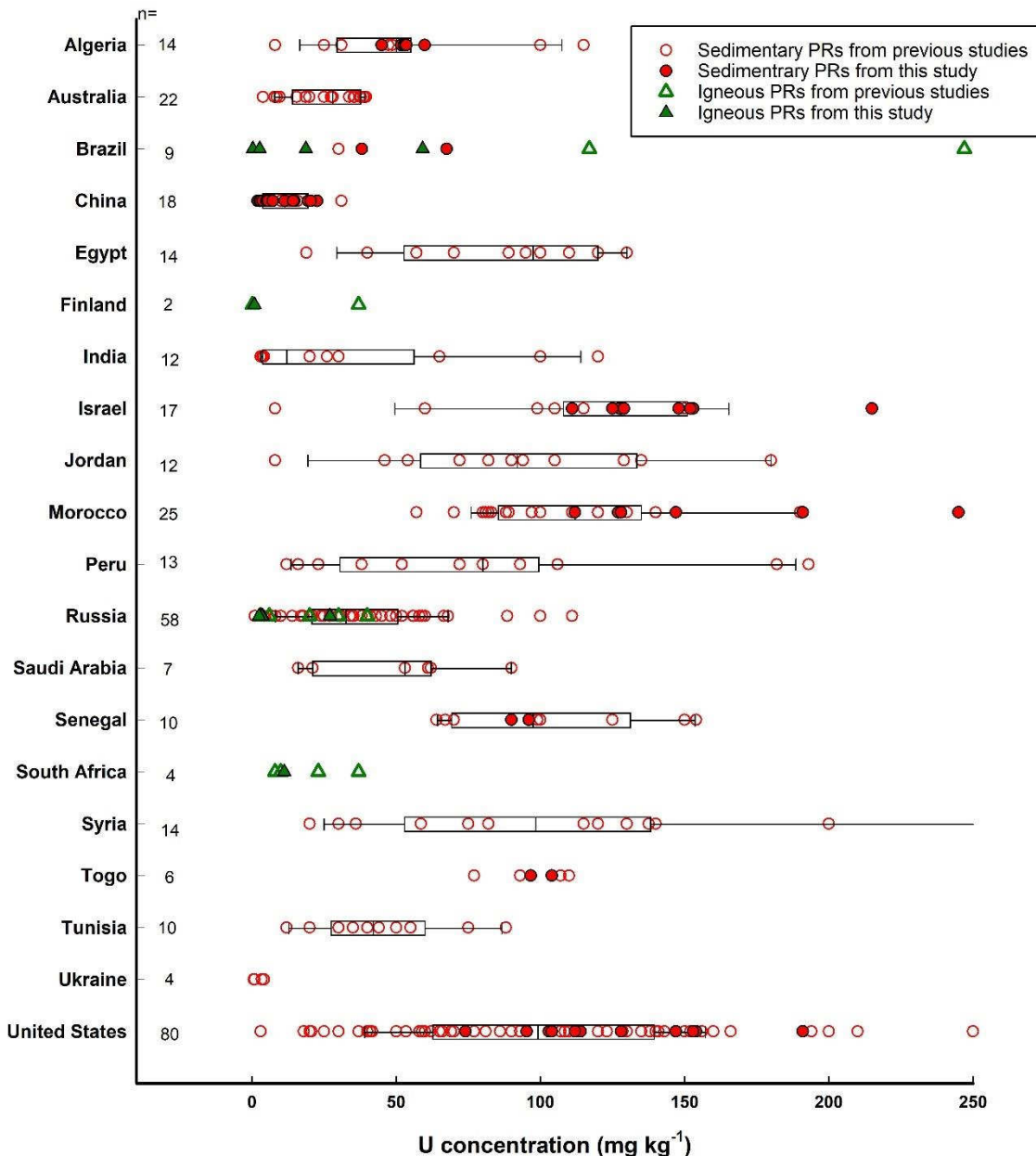


160
161 **Figure 1. Distribution of sedimentary and igneous phosphate deposits with respective**
162 **ages. (Age is the considering factor only for sedimentary PRs. Data source for**
163 **sedimentary and igneous phosphate deposits: Chernoff and Orris, 2002.)**
164

165 Igneous phosphates are a type of magmatic rock in which the element P was
166 incorporated into the crystal structure of apatite, which took place when the mineral
167 crystallized from the cooling melt (Pufahl and Groat, 2016). In general, the spatial and
168 temporal distributions of igneous apatite deposits are similar to those of alkaline

169 igneous rocks. Igneous phosphate deposits are also geographically fairly widespread
170 and range in age from Precambrian to Tertiary (Cook, 1984). The typical grade of P₂O₅
171 is 5-15 wt % and most associated phosphate deposits are small and not suitable for
172 commercial exploitation (Pufahl and Groat, 2016). The world's largest source of
173 igneous PRs stems from the Devonian Khibiny Alkaline Complex in Russia's Kola
174 Peninsula, contributing more than 50% of global igneous PRs use (Van Kauwenbergh
175 et al., 2010). The Jacupiranga deposits of Brazil, located at the edges of Paleozoic
176 basins and the Paleoproterozoic Palabora Complex deposit in South Africa, are the
177 two largest reserves of igneous PRs (Van Kauwenbergh et al., 2010; Pufahl and Groat,
178 2016).

179 The PRs from different countries generally show various degrees of enrichment with U
180 (Fig. 2). The data compilation reveals that igneous PRs, originating, for instance, from
181 Russia, China, South Africa and Finland, generally display U concentrations in the
182 range of 0.3-64 mg kg⁻¹, i.e. much lower than sedimentary PRs (0.6-390 mg kg⁻¹).
183 Among the examined sedimentary PRs, about 60% exhibited U concentrations from
184 80 to 150 mg kg⁻¹. Sedimentary PRs from Morocco, USA and Israel usually showed
185 relatively high U concentrations, with medians of 94, 116 and 129 mg kg⁻¹, respectively,
186 and also wide content range of 3-250, 57-245 and 8-215 mg kg⁻¹, respectively.
187 However, some sedimentary phosphate rock samples from Australia, Saudi Arabia,
188 and Turkey only contained U in concentrations in the range of 20-50 mg kg⁻¹. In
189 particular, the PRs originating from China show lower U concentrations in the range of
190 2.0 to 31 mg kg⁻¹ with a median of 11.4 mg kg⁻¹. According to this data base, PRs from
191 selected countries appear to exhibit a lower probability for U contamination than from
192 other countries; yet the range is large and U concentration alone cannot be used to
193 differentiate the origin of the different PRs.



194

Figure 2. Combination of scatter diagram and boxplot for U concentrations in phosphate rocks (PRs) from 20 countries. (Data include a total of 22 igneous and 339 sedimentary samples. Data sources: Altschuler et al., 1958; Altschuler et al., 1980; Banerjee et al., 1982; Baturin and Kochenov, 2001; Cevik et al., 2010; Cook et al., 1990; Cook, 1972; Dissanayake and Chandrajith, 2009; Dar et al., 2014; Hayumbu et al., 1995; Howard and Hough, 1979; Jallad et al., 1989; Khater et al., 2016; Levina et al., 1976; Makarov, 1963; Menzel, 1968; Pantelica et al., 1997; Parker, 1984; Pokryshkin, 1981; Sattouf, 2007; Schnug et al., 1996; Syers et al., 1986; Wakefield, 1980; Van Kauwenbergh, 1997; Zanin et al., 2000.)

204

205 3.1.2 Temporal distribution

206 In this study, the U content was normalized to the P₂O₅ content (as U/P₂O₅), in order
207 to take into consideration of the fact that U in PRs is generally associated with the
208 phosphoric phase (Brookfield et al., 2009; Föllmi, 1996; Lucas and Abbas, 1989).
209 Overall, the ratios of U/P₂O₅ in sedimentary PRs range from 0.02 to 17.7 in deposits of
210 all different ages, which shows that U deposition is highly variable with respect to
211 phosphorus content (Fig. 3). The median values of U/P₂O₅ of the PRs in each age
212 period decline in the deposits with increasing geological age of the deposits, with
213 median values of 0.1 for Precambrian PRs, 1.2 for Cambrian PRs, 2.9 for Ordovician-
214 Permian PRs, 2.6 for Triassic-Paleogene PRs and 3.5 for Neogene PRs, respectively.
215 The distributions of U/P₂O₅ in PRs of Ordovician-Permian, Triassic-Paleogene and
216 Neogene age are rather similar. In contrast, most Precambrian and Cambrian PRs
217 analyzed so far exhibit low U/P₂O₅ ratios below two. Obviously, the very ancient PRs
218 are characterized by low U/P₂O₅ ratios. A few previous studies also noticed the U-
219 depletion in ancient sedimentary PRs (Sokolov, 1996; Volkov, 1994). However, the
220 reasons for U depletion in ancient PRs were seldom investigated. In the following
221 sections the focus is on exploring the mechanisms for U deposit in PRs.

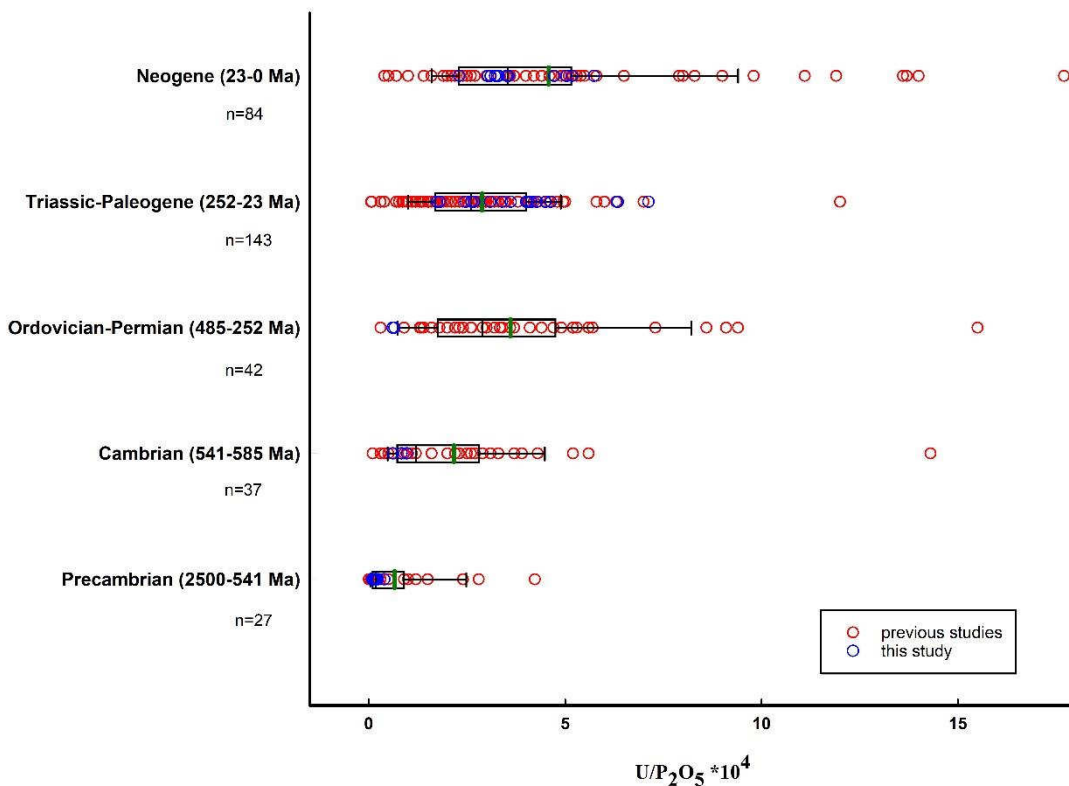
222

223 **3.2 Mechanisms of various deposition processes of U in phosphate rocks**

224 **3.2.1 U speciation in PRs**

225 Apatite is the most abundant phosphate mineral. It is believed that U is mainly
226 associated with apatite as radioactivity detected in phosphate nodules mostly
227 originates from apatite. In addition, U contents extracted from various PRs samples
228 are essentially the same when only apatite or apatite plus silicates is dissolved
229 (Altschuler, 1958). Igneous apatite rocks consist of three primary mineral forms:
230 chlorapatite [Ca₅(PO₄)₃Cl], hydroxylapatite [Ca₅(PO₄)₃OH], and fluorapatite
231 [Ca₅(PO₄)₃F] (Jarvis, 1995). In sedimentary apatites, the main ore mineral is francolite

232 [Ca_{10-a-b}Na_aMg_b(PO₄)_{6-x}(CO₃)_{x-y-z}(CO₃·F)_{x-y-z}(SO₄)_zF₂] (Jarvis, 1995; Petr, 2016). Two
 233 states of U can be present in these PRs either as UO₂, UF₄ or Ca(UO₂)₂(PO₄)₂8H₂O
 234 phases, or as isolated U⁴⁺ ions or UO₂²⁺ radicals adsorbed on mineral surfaces or
 235 within internal discontinuities (Hendricks and Hill, 1950). It may also be substituted
 236 structurally in apatite, as U⁴⁺ by replacement of Ca²⁺, owing to the virtually identical
 237 ionic radii of U⁴⁺ (1.05 Å) and Ca²⁺ (1.06 Å) (Baturin and Kochenov et al., 2000). Uranium
 238 in the structure of apatite dominates as U (IV). The present of U (VI) fixed as a surface-
 239 coordinated uranyl pyrophosphate is derived largely from post-depositional oxidation
 240 of U(IV) (Altschuler, 1958). In addition, the studies on submarine phosphorite also
 241 indicate the observed U(VI) content are not solely the product of surface oxidation and
 242 that U is probably incorporated in apatite in both oxidation state (Kolodny and Kaplan,
 243 1970; Burnett and Veeh, 1977).



244
 245 **Figure 3. Distribution of U/P₂O₅ in sedimentary PRs during geologic time from**
 246 **Precambrian to Holocene. The plot is a combination of scatter diagram and boxplot. The**
 247 **green lines are mean values for each period of geologic time.**

248

249 3.2.2 Variation of U deposition in igneous and sedimentary PRs

250 Differences in U/P₂O₅ ratios reflect to a large degree the diversities in the formation
251 mechanisms for igneous and sedimentary PRs. Apatite deposits of igneous origin
252 occur as intrusive masses or sheets, as hydrothermal veins or disseminated
253 replacements, or as marginal differentiations along or near the boundaries of intrusions,
254 or as pegmatites (McKelvey, 1967). It has been reported that most igneous apatites
255 contain U concentration between 40-80 mg kg⁻¹ (Altschuler et al., 1958). Most recently
256 Windmann (2019) reports from a much larger sample population a geometric mean of
257 7.56 mg kg⁻¹ with a variation coefficient of 119%. The amount of U available to apatite
258 largely depends on special environmental circumstances, presumably, the production
259 of U (IV). The occurrence of U in igneous apatite is governed by the equilibrium
260 conditions prevailing in the magma during the precipitation of apatite (Altschuler et al.,
261 1958). The amount of U available to igneous apatite is regulated by apatite's capacity,
262 as well as the capacities of the other hosts coextensive with U and thus reflects the
263 total equilibrium in the magma (Altschuler et al., 1958). In contrast to igneous apatite,
264 the occurrence of U in marine sedimentary apatite is not governed solely by the
265 equilibrium condition in the ocean, but also by the subsequent secondary enrichment
266 processes during marine reworking (Baturin and Kochenov, 2001; Altschuler et al.,
267 1958). The enrichment of U in sedimentary apatite implies that apatite has acquired
268 and sequestered additional U from the sea water. Uranium is removed from the
269 seawater by diffusion across the sediment-water interface. Dissolved U is drawn into
270 the anoxic zone of sediment layer along a concentration gradient caused by the
271 precipitation of U(VI) to U(IV). This transformation is induced by microbially mediated
272 dissolution of manganese and iron oxides, and sulfate reduction (Klinkhammer and
273 Palmer, 1991; Soudry et al., 2002). The presence of apatite can actively affect the

274 course of the reduction reactions ($(\text{UO}_2)^{+2} + \text{reductant} \leftrightarrow \text{U}^{+4} + \text{oxidized reductant}$), by
275 sequestering U (IV), thereby a continuous supply of U(IV) (Altschuler et al., 1958).

276

277 3.2.3 Mechanism of U variation in sedimentary PRs

278 Even if U is enriched in sedimentary PRs, the reasons for considerable low U
279 concentrations in ancient PRs are complex. They may be a comprehensive result of
280 three factors: i) the evolution of U in the earth during geological history, ii) different
281 paleogeographic features, and iii) weathering and catagenesis, which all affect the fate
282 of U in phosphate deposits, as outlined below.

283 Geochemical evolution of U along the geologic units

284 The U concentration in sediments reflects the size of the local and perhaps global
285 marine environment U reservoir (Partin et al., 2013). The geochemical evolution of U
286 in marine is affected by two major events: the development of an oxygenated
287 atmosphere about 2.2 billion years ago and the development of land plants at about
288 0.4 billion years ago (Cuney, 2010). Before oxygenation started, the reduced
289 conditions in the absence of O₂ resulted in low solubility and low concentration of U in
290 water (Partin et al., 2013). The lack of U enrichment in ancient PRs deposits in this
291 study confirms the low concentration of soluble U in marine waters. In the period of
292 2.3-0.45 Ga, during and after the Great Oxidation Event (GOE) when oxygen increased
293 near to the present atmospheric level, oxidative processes took place in terrestrial
294 environments and the continental fluxes of dissolved U to the oceans increased
295 dramatically (Holland, 1984). The last period was from 0.45 Ga to the present, when
296 the Earth was colonized by plants. Uraninite and coffinite were precipitated from the
297 U-rich near-surface waters into the oxygenated and organic-rich continental sediments;
298 thus, total U concentrations in the sediments increased significantly (Cuney, 2010). As
299 a consequence, higher U concentrations were found in younger PRs.

300 Paleogeographic features

301 The U depletion in ancient phosphorites was additionally caused by the
302 paleogeographic features of relevant basins (such as in Asia and Africa), where U
303 influx was considerably less pronounced during the phosphorus influx into the
304 phosphate accumulation zones (Stephens and Carroll, 1999; Baturin and Kochenov,
305 2001). In contrast, the U-enrichment in later geologic time units was associated with
306 paleogeographic reconstructions upon upwelling, which promoted both U and P
307 deliveries into the shallow shelves (Baturin and Kochenov, 2001). Additionally, the
308 process of U accumulation is believed to be related to sedimentary reducing conditions
309 (Avital et al., 1983; Altschuler, 1958), where soluble U(VI) was reduced to insoluble
310 U(IV) and deposited in the sediments. Elevated loads of organic matter led to reduced
311 sedimentary conditions (McManus et al., 2005) turning them into a significant sink for
312 U (Altschuler, 1958).

313 Weathering and catagenesis

314 Apart from the geochemical conditions during U influx and accumulation, weathering
315 and catagenesis can control the residence time of U within the reservoir (Zanin et al.,
316 2000). The effects of subaerial weathering remove apatite constituents from the apatite
317 structure. Consequently, apatite decomposes, and soluble mineral phases and
318 speciation of trace elements, such as U, are lost during weathering (Howard and
319 Hough 1979; Zanin et al., 1985). In addition, the composition and texture of
320 sedimentary apatite could be essentially modified in catagenesis (Zanin et al., 1985).
321 The catagenesis processes correspond to remove isomorphic impurities from
322 carbonateapatite, such as carbonate ions, isomorphic trace elements (e.g. Sr, Cd, U),
323 sodium, and H_2O^+ (Zanin et al., 1985). Therefore, the U concentrations in ancient PRs
324 are relatively low, since the ancient phosphate rocks were exposed to catagenesis for
325 a longer period (Baturin and Kochenov, 2001).

326

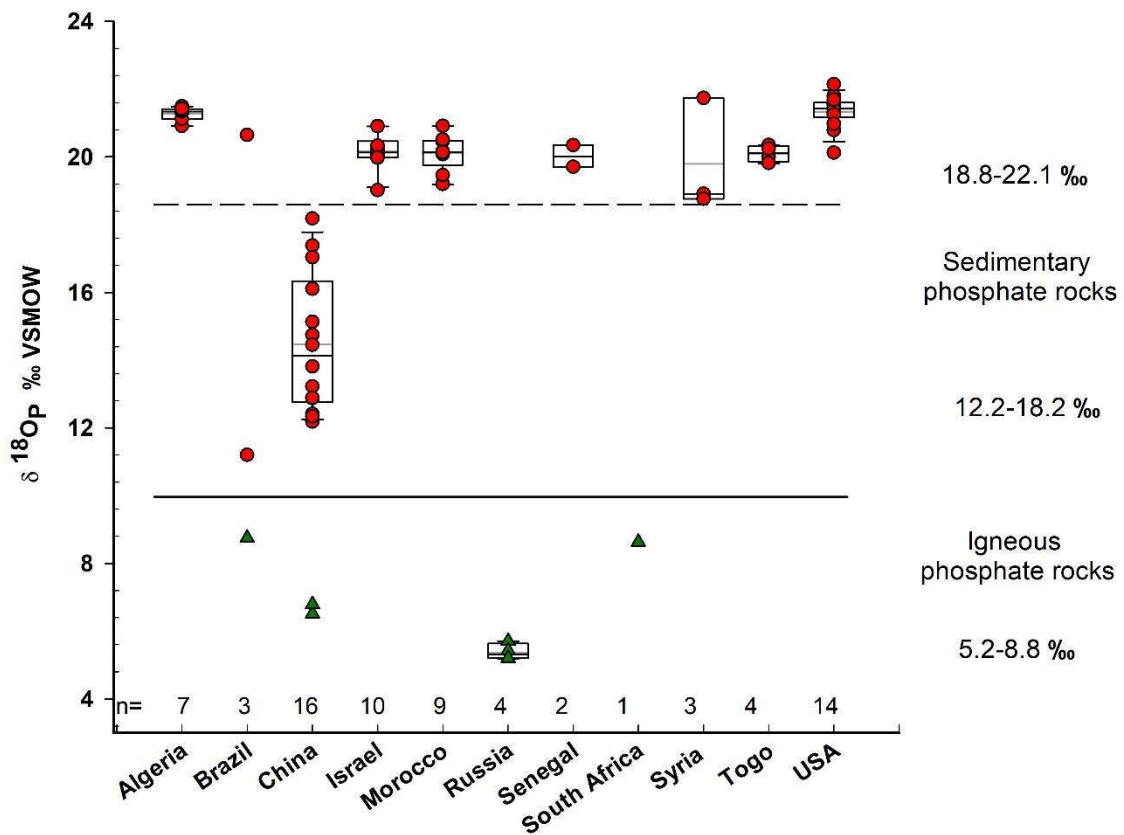
327 **3.3 Oxygen isotope signature in phosphate deposits**

328 As all the processes mentioned so far interact with each other, with unclear relations
329 to the origins of phosphates in PRs, the oxygen isotope natural abundances of
330 phosphates ($\delta^{18}\text{O}_p$) is included as an additional indicator to distinguish PRs of different
331 origins and with different U concentrations.

332 3.3.1 Oxygen isotope fingerprint of phosphate rocks of various origins

333 The O isotope compositions of the phosphates in the PRs are variable, thus
334 fingerprinting their deposits (Fig. 4). In general, three different groups of PRs differing
335 in their $\delta^{18}\text{O}_p$ natural abundance values can be differentiated: 1) igneous PRs from
336 Brazil, China, Russia and South Africa ($\delta^{18}\text{O}_p \leq 8.8\text{ ‰}$), 2) sedimentary PRs from China
337 and Brazil ($\delta^{18}\text{O}_p 12.2 - 18.2\text{ ‰}$), and 3) sedimentary PRs from Algeria, Israel, Morocco,
338 Russia, Senegal, South Africa, Syria, Togo and the USA ($\delta^{18}\text{O}_p \geq 18.8\text{ ‰}$; Fig. 4).

339 .



340

341 **Figure 4. Variation of oxygen isotope composition ($\delta^{18}\text{O}_p$) in phosphate rocks (PRs) from**
 342 **different countries.**

343

344 All igneous PRs show relatively low $\delta^{18}\text{O}_p$ values (5.2 - 8.8‰), which are comparable
 345 in magnitude with the $\delta^{18}\text{O}_p$ values of igneous apatite reported previously (Taylor,
 346 1962). In contrast, larger and a wider range of $\delta^{18}\text{O}_p$ values (from 12.2 to 22.1‰) are
 347 found in sedimentary PRs. Notably, the $\delta^{18}\text{O}_p$ values of sedimentary PRs from China,
 348 as well as one sample from Brazil, show an intermediate range of $\delta^{18}\text{O}_p$ values (12.2-
 349 18.2‰). The other sedimentary PRs of this study exhibit a considerable narrow range
 350 of $\delta^{18}\text{O}_p$ from 18.8 to 22.1‰.

351

352 3.3.2 Mechanisms causing various $\delta^{18}\text{O}_p$ in phosphate rocks

353 The final $\delta^{18}\text{O}_p$ isotope composition in PRs largely depends on that of the source water
 354 and the $\delta^{18}\text{O}_p$ values within these rocks may be then regarded as reflections of their

355 crystallization history (Taylor, 1962). Potential sources of fluids involved in the
356 formation or alteration of phosphate deposits include magmatic water, meteoric water
357 and ocean water. These three are characterized by specific $\delta^{18}\text{O}_w$ values. Magmatic
358 water which has never been in contact with the hydrosphere has $\delta^{18}\text{O}_w$ values from 5
359 to 8 ‰ (Shepherd et al., 1985). The relatively low $\delta^{18}\text{O}_p$ values of igneous PRs in this
360 study are close to these low $\delta^{18}\text{O}_w$ values of magmatic water (Kusakabe and
361 Matsubaya, 1986). In addition, limited fractionation will take place in the high
362 temperature magma during the precipitation of the apatite. Therefore, apatite in
363 igneous rocks may retain the same low $\delta^{18}\text{O}$ as the magmatic water. The variation of
364 $\delta^{18}\text{O}_p$ values in igneous PRs reflects the range of temperatures at which the fluids were
365 produced.

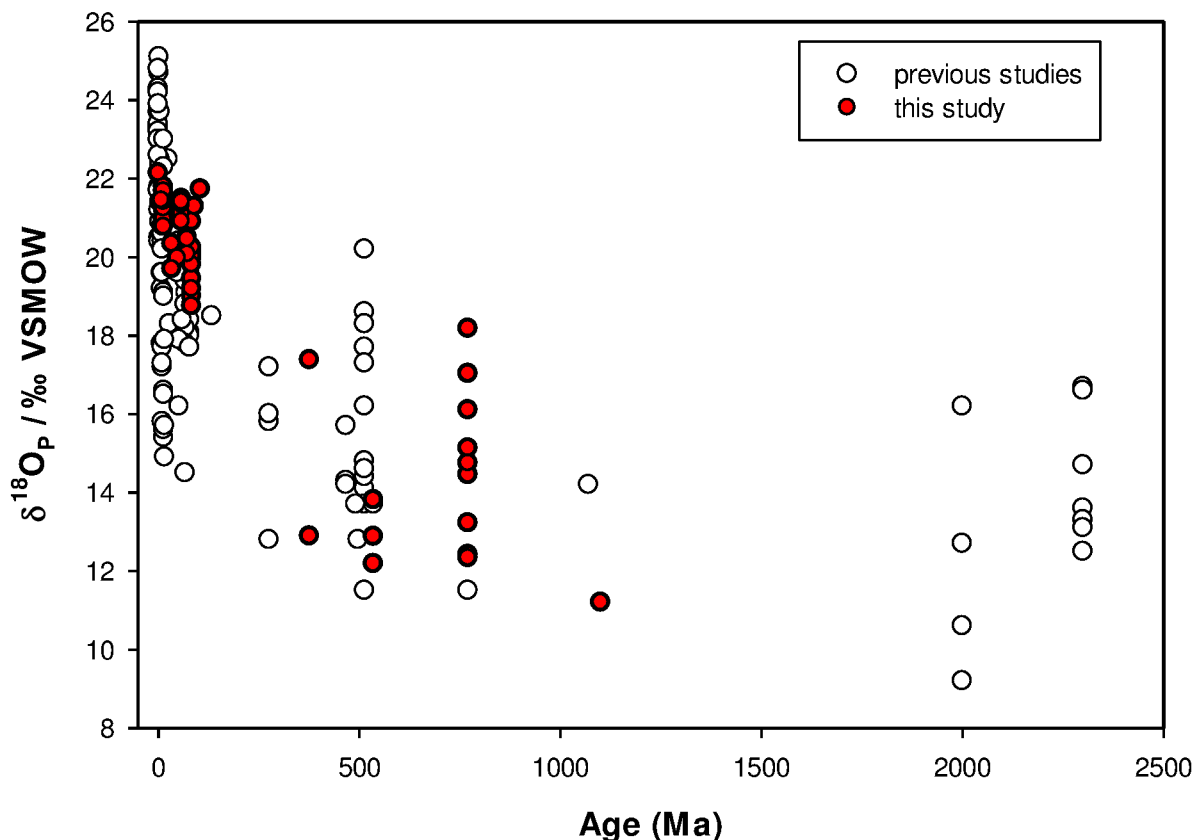
366 The $\delta^{18}\text{O}_p$ values of sedimentary PRs in this study are in the range of marine
367 sedimentary phosphate (9.2-23.9‰) as reported previously by Shemesh et al. (1988).
368 The ultimate fluid origin of sedimentary materials involves trapped seawater, or
369 evolved meteoric water (Fayek, et al., 2011). The details of $\delta^{18}\text{O}$ in seawater will be
370 discussed in the following. Meteoric waters, in turn, are abundant in rivers, lakes,
371 glaciers and groundwater. They usually exhibit elevated $\delta^{18}\text{O}$ values due to various
372 degrees of water-rock interactions (Shepherd et al., 1985). In addition, the geographic
373 (such as island effect) (Tang et al., 1998) and climatic parameters (e.g. latitude,
374 elevation, distance from the coast) correlated with the $\delta^{18}\text{O}_p$ values (Dutton et al., 2005).
375 These different influences thus explain the large variations in O isotopic compositions,
376 as well as the variations of $\delta^{18}\text{O}_p$ values in most of the analyzed sedimentary PRs.
377 The reasons for the variation of lower $\delta^{18}\text{O}_p$ values in sedimentary PRs also deserve
378 to be considered. It can be noted that low $\delta^{18}\text{O}_p$ values of the sedimentary PRs were
379 accompanied by older ages of formation. For instance, the sedimentary PRs from
380 China which formed in Ediacaran-Cambrian (485-635 Ma) and Devonian (359-419 Ma)

periods (Cook and Shergold, 2005; He and Zhou, 2015), have lower $\delta^{18}\text{O}_p$ values. Younger sedimentary PRs from Algeria, Israel, Morocco, Senegal, South Africa, Syria and Togo, formed in Cretaceous-Paleogene (56-145 Ma) times (Notholt, 1986), on the other hand, exhibited relatively higher $\delta^{18}\text{O}_p$ values in the range of 18.7-21.4‰. The youngest PRs in this study were from the USA, and also exhibited the highest $\delta^{18}\text{O}_p$ values, although within a narrow range (20.1-21.8‰; Fig. 4). The findings indicate that there is a clear relation between the $\delta^{18}\text{O}_p$ values and the age of the sedimentary PRs. This conclusion is supported by earlier suggestions of, e.g. Longinelli and Nuti (1968), and Shemesh et al. (1988), who found that $\delta^{18}\text{O}_p$ values decreased sharply from recent to Cretaceous times (66-145 Ma), and decreased further with a gentle slope to the Precambrian (541 Ma) (Fig. 5). The underlying mechanisms, however, are still a matter of debate, particularly because there is no consensus yet to whether it was temperature or the $\delta^{18}\text{O}$ value of the ancient ocean water that led to low $\delta^{18}\text{O}_p$ values in ancient rocks (Blake et al., 2010; Longinelli and Nuti, 1968; Shemesh et al., 1983, 1988). Three main explanations have been offered: 1) ocean water temperatures must have decreased from ancient to recent times (Knauth and Epstein, 1976; Knauth and Lowe, 2003; Shemesh et al., 1983), 2) the changing $\delta^{18}\text{O}$ value of sea water over time (e.g. Chase and Perry, 1972), 3) increasing $\delta^{18}\text{O}_p$ values from ancient to recent times caused by post-depositional alterations (Shemesh et al., 1983).

The opinion that ancient PRs were deposited under high temperatures has been put forward by many studies (Shemesh et al., 1983; Piper and Kolodny, 1987; Blake et al., 2010). Such higher temperatures could have been either a reflection of global phenomena, i.e. of warmer oceans in the geological past, or of a shift in the site of phosphate rocks formation in the ocean (Kolodny and Luz, 1992). Assuming that the $\delta^{18}\text{O}_w$ of the sea water was about 0 ‰ and that this value was maintained over geologic timescales in the absence of glacial periods (Muehlenbachs, 1998), the sedimentary

407 PRs should thus have formed at an isotopic equilibrium with $\delta^{18}\text{O}_w = 0\text{\textperthousand}$. The
408 calculated ocean temperatures of the Ediacaran-Cambrian (485-635 Ma), Devonian
409 (359-419 Ma), Cretaceous-Paleogene (56-145 Ma), and Neogene-Quaternary (0.01-
410 23 Ma) in this study would then have been 42.2 °C, 36.7 °C, 23.9 °C and 19.6 °C,
411 respectively. This indicates that the temperature of the ocean slowly decreased with
412 time and the evolution of the Earth. An even higher temperature (> 60 °C) has been
413 proposed for Archean and early Proterozoic waters (Knauth and Epstein, 1976; Robert
414 and Chaussidon, 2006).

415 The $\delta^{18}\text{O}_w$ values of the ocean can only change very slowly, since the residence time
416 of water in the ocean is very long compared to hydrothermal circulation (Land and
417 Lynch, 1996), and rates of chemical weathering on the continents are also slow. Hence,
418 the seawater $\delta^{18}\text{O}_w$ value is assumed to have been fairly constant over time, buffered
419 by hydrothermal and weathering processes at mid-ocean ridges to a $\delta^{18}\text{O}_w$ value of
420 about 0‰ (Standard Mean Ocean Water, SMOW) (e.g. Muehlenbachs, 1998; Holland,
421 1984). Hren et al. (2009) disagreed with this view and considered that, the $\delta^{18}\text{O}_w$ value
422 could have been as low as -10 to -13‰ in the Archaean ocean with a subsequent
423 increase to present-day values. However, Blake et al. (2010) argued that based on the
424 equation of Longinelli and Nuti (1973) mentioned above, such a conclusion would imply
425 that the $\delta^{18}\text{O}_p$ values of Archaean marine phosphate would have been formed at an
426 unrealistic ocean temperature of -8 °C to -30 °C. This conclusion favored the former
427 interpretation that the increase of $\delta^{18}\text{O}_p$ with decreasing geological age of the PRs
428 most likely reflects the progressive cooling of sea temperatures during Earth's history.
429 In any case, there was a coincidental 'co-evolution' (but not coupled) of $\delta^{18}\text{O}_p$ signature
430 in PRs and their U concentration, as a function of sedimentary PRs' age.



431

432 **Figure 5. Oxygen isotope in phosphates ($\delta^{18}\text{O}_p$) as related to the geological age of the**
 433 **sedimentary phosphate rocks (Data for circles are from Shemesh et al., 1983, 1988 and**
 434 **data for red points are from this study).**

435

436 It should be noted that despite a likely wholesale lowering of $\delta^{18}\text{O}_p$ values in older
 437 marine PRs, the ranges of $\delta^{18}\text{O}_p$ values found for the PRs in this study are broad, even
 438 for those originating from a given geographic region and geologic time unit. It seems
 439 therefore likely that additional effects by post-depositional isotopic exchange altered
 440 the $\delta^{18}\text{O}_p$ value between the O in phosphate and that in the surrounding water. Earlier
 441 work by Longinelli and Nuti (1968) proposed that post-depositional processes could
 442 have shifted the $\delta^{18}\text{O}_p$ values of sedimentary rocks to lower levels, since alteration
 443 commonly occurred in the presence of ^{18}O -depleted meteoric waters or at elevated
 444 temperature (Jaffres et al., 2007). Moreover, $\delta^{18}\text{O}_p$ studies of fish debris, pointed to
 445 considerably larger values than in associated phosphate rocks, indicating the possible

446 existence of a significant post-depositional isotopic exchange in the latter (Kastner et
447 al., 1990).

448

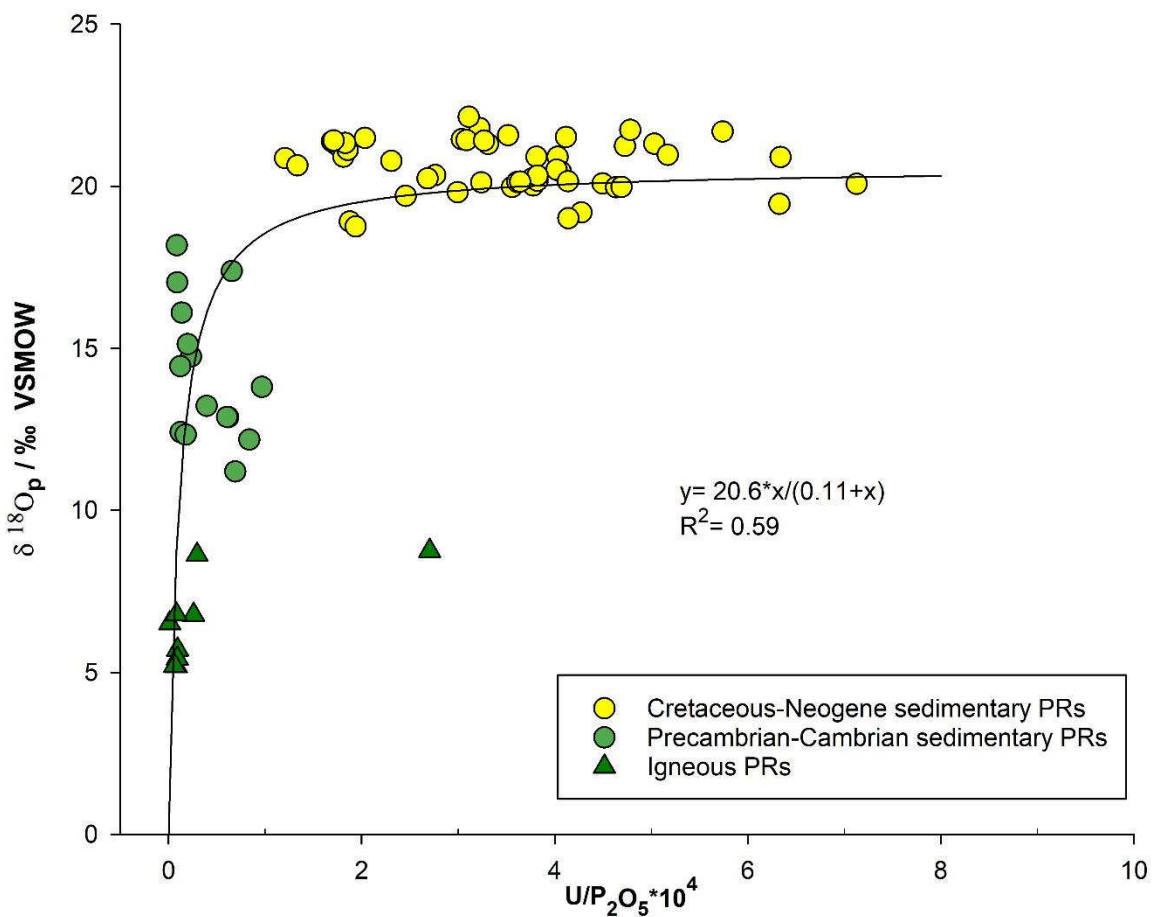
449 **3.4. Relationship between the U/P₂O₅ and δ¹⁸O_p in phosphate rocks**

450 The U/P₂O₅ and δ¹⁸O_p values showed a clearly positive correlation (Fig. 6), pointing to
451 some kind of ‘co-evolution’ of U history and oxygen isotope exchange in PRs. The
452 igneous rocks clustered at the lower end of the curve, thus clearly distinguishing these
453 PRs from the sedimentary ones. Old sedimentary PRs (Precambrian-Cambrian) with
454 low δ¹⁸O_p values also displayed lower U/P₂O₅ ratios. The younger sedimentary PRs
455 (Cretaceous-Neogene), in turn, exhibited a wide range of U/P₂O₅ ratios with relatively
456 high δ¹⁸O_p values.

457 In igneous PRs, the low U concentration can be attributed to the lack of secondary U
458 enrichment processes (Alschuler, 1958), whereas the low δ¹⁸O_p values in PRs are
459 likely due to a low concentration of ¹⁸O in magmatic water and the limited oxygen
460 isotopic fractionations in high temperature magmatic water (Taylor, 1968). In contrast,
461 in sedimentary PRs, the time trend for U/P₂O₅ ratios and δ¹⁸O_p values reflects a
462 coincidence of paleoclimate and paleogeographic features. A low ratio in PRs indicates
463 either that little U was further precipitated into francolite or that the U was released
464 from the apatite lattices as a result of intensive post-depositional diagenetic processes.
465 The latter process may also lower the δ¹⁸O_p values (Shemesh et al., 1983). It is hard
466 to find direct coupling of processes involved in U deposition and oxygen exchange, but
467 findings rather indicate a time-dependent coincidence of processes altering U content
468 and δ¹⁸O_p signatures in a similar direction.

469 In summary, the results reported in this paper support the hypothesis that there is a
470 co-evolution of δ¹⁸O_p and U/P₂O₅ ratios in PRs across different geologic time units.
471 Plotting both parameters against each other may provide a novel tool for PR dating,

472 potentially supplementing existing dating tools, which are frequently valid for selected
 473 time windows only, in the case of Sr and U isotopes, for instance, precisely only for the
 474 0-20 Ma and 0-1.2 Ma age range, respectively. On the other hand, the data clearly
 475 show that selecting mineral P fertilizers on the basis of the geological origin (igneous
 476 versus sedimentary) and age (Precambrian-Cambrian versus Cretaceous to Neogene)
 477 of their PRs may help to find $\delta^{18}\text{O}_p$ signatures of fertilizer P that differ from that of soil
 478 and plants and could thus be used as a tracer for elucidating the biological cycling of
 479 fertilizer P in the terrestrial environment (Tamburini et al., 2012; Amelung et al., 2015;
 480 Bauke et al., 2018).



481

482 **Figure 6. Correlation between oxygen isotope composition of phosphate ($\delta^{18}\text{O}_p$) and**
 483 **$\text{U}/\text{P}_2\text{O}_5$ in phosphate rocks (PRs).**

484

485 **4. Conclusion**

486 To prevent and explain different levels of U contamination in agricultural soils, this work
487 provides a comprehensive overview of U levels in various PRs worldwide and the
488 underlining mechanisms of U accrual. We linked these data to information on the
489 oxygen isotope composition of PRs, which provides additional information on the
490 related genesis of P in these rocks. In soil, oxygen isotope abundance measurements
491 of phosphates provide additional information on the efficiency of soil P cycling; yet,
492 linking the latter to the origin of P fertilizers is still in its fledging stages (Tamburini et
493 al., 2012; Amelung et al., 2015; Helfenstein et al., 2018).

494 The comprehensive overview of U levels in various PRs not only confirmed that
495 igneous PRs contained lower levels of U than sedimentary PRs, but also that older
496 sedimentary PRs (Precambrian-Cambrian) have less U than younger ones
497 (Ordovician-Neogene). In addition, $\delta^{18}\text{O}_\text{P}$ distinguished the PRs deposits of: 1) igneous
498 PRs ($\delta^{18}\text{O}_\text{P} = 5.2$ to $8.8\text{\textperthousand}$, e.g. from Russia), 2) old sedimentary PRs ($\delta^{18}\text{O}_\text{P} = 12.2$ to
499 $18.2\text{\textperthousand}$, e.g. from China), and 3) younger sedimentary PRs ($\delta^{18}\text{O}_\text{P} = 18.8$ to $22.1\text{\textperthousand}$, e.g.
500 from the USA). Finally, the differences of U levels in PRs were mirrored by the $\delta^{18}\text{O}_\text{P}$
501 signatures of the PRs, thus highlighting both their ‘co-evolution’, and inter changeability
502 as a tracer of temporal or process changes in global PRs.

503

504 **Acknowledgements**

505 The authors would like to acknowledge the colleagues in Julius Kühn-Institut, Germany,
506 for the help in collecting the phosphate rocks. They also express their sincere thanks
507 to Dr. Tamburini and the colleagues in her group at ETH, and Dr. Bauke and Ye Wang
508 at Bonn University, who helped establish and test the purification method for oxygen
509 isotope analysis. We also want to Holger Wissel, in IBG-3, Forschungszentrum Jülich
510 for performing the oxygen stable isotope analysis. This study was supported by the
511 Chinese Scholarship Council (CSC201506350148).

512

513 **References**

- 514 Altschuler, Z. S., 1958. Geochemistry of uranium in apatite and phosphorite. US
515 Geological Survey. 314-D: 45–90.
- 516 Altschuler, Z. S., 1980. The geochemistry of trace elements in marine phosphorites:
517 Part I. Characteristic abundances and enrichment. The Society of Economic
518 Paleontologists and Mineralogist Special Publication, 29: 19–30.
- 519 Amelung, W., Antar, P., Kleeberg, I., Oelmann, Y., Luecke, A., Alt, F., Lewandowski,
520 H., Pätzold, S. and Barej, J., 2015. The $\delta^{18}\text{O}$ signatures of HCl-extractable soil
521 phosphates: methodological challenges and evidence of the cycling of biological
522 P in arable soil. European Journal of Soil Science, 66 (6): 965-972.
523 <https://doi.org/10.1111/ejss.12288>
- 524 Avital, Y., Starinsky, A. and Kolodny, Y., 1983. Uranium geochemistry and fission-track
525 mapping of phosphorites, Zefa field, Israel. Economic Geology, 78(1): 121-131.
526 <https://doi.org/10.2113/gsecongeo.78.1.121>
- 527 Banerjee, D., Khan, M., Srivastava, N. and Saigal, G., 1982. Precambrian phosphorites
528 in the Bijawar rocks of Hirapur-Bassia areas, sagar district, madhya pradesh,
529 India. Mineralium Deposita, 17, 349-362. <https://doi.org/10.1007/BF00204465>
- 530 Baturin, G. and Kochenov, A., 2001. Uranium in phosphorites. Lithology and mineral
531 resources, 36(4): 303-321. <https://doi.org/10.1023/A:1010406103447>
- 532 Bauke, S.L., von Sperber, C., Tamburini, F., Gocke, M., Honermeier, B., Schweitzer,
533 K., Baumecker, M., Don, A., Sandhage-Hofmann, A. and Amelung, W., 2018.
534 Subsoil phosphorus is affected by fertilization regime in long-term agricultural
535 experimental trials. European Journal of Soil Science, 69(1): 103-112.
536 <https://doi.org/10.1111/ejss.12516>

- 537 Bigalke, M., Schwab, L., Rehmus, A., Tondo, P. and Flisch, M., 2018. Uranium in
538 agricultural soils and drinking water wells on the Swiss Plateau. Environment
539 Pollution. 233: 943-951. <https://doi.org/10.1016/j.envpol.2017.09.06>
- 540 Blake, R.E., Chang, S.J. and Lepland, A., 2010. Phosphate oxygen isotopic evidence
541 for a temperate and biologically active Archaean ocean. Nature, 464(7291): 1029.
542 <https://doi.org/10.1038/nature08952>
- 543 Brookfield, M., Hemmings, D. and Van Straaten, P., 2009. Paleoenvironments and
544 origin of the sedimentary phosphorites of the Napo Formation (Late Cretaceous,
545 Oriente Basin, Ecuador). Journal of South American Earth Sciences, 28(2): 180-
546 192. <https://doi.org/10.1016/j.jsames.2009.02.004>
- 547 Burnett, W.C. and Veeh, H.H., 1977. Uranium-series disequilibrium studies in
548 phosphorite nodules from the west coast of South America. Geochimica et
549 Cosmochimica Acta, 41(6), pp.755-764.
- 550 Cevik, U., Baltas, H., Tabak, A. and Damla, N., 2010. Radiological and chemical
551 assessment of phosphate rocks in some countries. Journal of hazardous
552 materials, 182(1-3): 531-535. <https://doi.org/10.1016/j.jhazmat.2010.06.064>
- 553 Chase, C. G. and Perry, E. C., 1972. The oceans: growth and oxygen isotope evolution.
554 Science, 177(4053), 992-994. <https://doi.org/10.1126/science.177.4053.992>
- 555 Chernoff, C.B. and Orris, G.J., 2002. Data set of world phosphate mines, deposits, and
556 occurrences: Part A. geologic data; Part B. location and mineral economic data.
557 2002-156. <https://doi.org/10.3133/ofr02156>
- 558 Cook, P. J. 1972. Petrology and geochemistry of the phosphate deposits of northwest
559 Queensland, Australia. Economic Geology, 67, 1193-1213.
560 <https://doi.org/10.2113/gsecongeo.67.8.1193>

- 561 Cook, P., O'Brien, G., Burnett, W. and Riggs. S., 1990. Neogene to Holocene
562 phosphorites of Australia. In: Burnett, W.C. and Riggs, S.R. (Eds). Phosphate
563 Deposits of the World, Cambridge University Press, Cambridge, pp. 98-115.
- 564 Cook, P.J. and Shergold, J.H., 2005. Phosphate Deposits of the World: Volume 1:
565 Proterozoic and Cambrian Phosphorites. Cambridge University Press.
- 566 Cook, P.J., 1984. Spatial and temporal controls on the formation of phosphate
567 deposits- a review, Phosphate minerals. Springer, pp. 242-274.
568 https://doi.org/10.1007/978-3-642-61736-2_7
- 569 Cuney, M., 2010. Evolution of uranium fractionation processes through time: driving
570 the secular variation of uranium deposit types. Economic Geology, 105(3): 553-
571 569. <https://doi.org/10.2113/gsecongeo.105.3.553>
- 572 Dar, S.A., Khan, K.F., Khan, S.A., Mir, A.R., Wani, H., Balaram, V., 2014. Uranium (U)
573 concentration and its genetic significance in the phosphorites of the
574 Paleoproterozoic Bijawar Group of the Lalitpur district, Uttar Pradesh, India..
575 Arabian Journal of Geosciences 7 (6), 2237–2248. doi.org/10.1007/s12517-013-
576 0903-8.
- 577 Dissanayake, C. B. and Chandrajith, R., 2009. Phosphate mineral fertilizers, trace
578 metals and human health. Journal of the National Science Foundation of Sri
579 Lanka, 37(3): 153-165.
- 580 Dutton, A., Wilkinson, B. H., Welker, J. M., Bowen, G. J. and Lohmann, K. C., 2005.
581 Spatial distribution and seasonal variation in $^{18}\text{O}/^{16}\text{O}$ of modern precipitation and
582 river water across the conterminous USA. An International Journal, 19(20),
583 4121-4146. <https://doi.org/10.1002/hyp.5876>
- 584 Fayek, M., Horita, J. and Ripley, E.M., 2011. The oxygen isotopic composition of
585 uranium minerals: A review. Ore Geology Reviews, 41(1):1-21.
586 <https://doi.org/10.1016/j.oregeorev.2011.06.005>

- 587 Föllmi, K., 1996. The phosphorus cycle, phosphogenesis and marine phosphate-rich
588 deposits. *Earth-Science Reviews*, 40(1-2): 55-124. [https://doi.org/10.1016/0012-8252\(95\)00049-6](https://doi.org/10.1016/0012-8252(95)00049-6)
- 589
- 590 Hayumbu, P., Haselberger, N., Markowicz, A. and Valkovic, V., 1995. Analysis of rock
591 phosphates by x-ray fluorescence spectrometry. *Applied radiation and isotopes*,
592 46(10): 1003-1005. [https://doi.org/10.1016/0969-8043\(95\)00206-S](https://doi.org/10.1016/0969-8043(95)00206-S)
- 593 He, G., and Zhou, Y., 2015. Geology of Phosphate Rock in China: Distribution, Rock
594 Type and Metallogenic Perspective. *Global Environmental Research*, 19, 91-96.
- 595 Helfenstein, J., Tamburini, F., von Sperber, C., Massey, M.S., Pistocchi, C., Chadwick,
596 O.A., Vitousek, P.M., Kretzschmar, R. and Frossard, E., 2018. Combining
597 spectroscopic and isotopic techniques gives a dynamic view of phosphorus
598 cycling in soil. *Nature communications*, 9(1): 3226.
- 599 Hendricks, S. and Hill, W., 1950. The nature of bone and phosphate rock. *Proceedings*
600 of the National Academy of Sciences, 36(12): 731-737.
601 <https://doi.org/10.1073/pnas.36.12.731>
- 602 Holland, H.D., 1984. The chemical evolution of the atmosphere and oceans. Princeton
603 University Press.
- 604 Howard, P. and M. Hough., 1979. On the geochemistry and origin of the D Tree,
605 Wonarah, and Sherrin Creek phosphorite deposits of the Georgina Basin,
606 northern Australia. *Economic Geology*, 74, 260-284.
607 <https://doi.org/10.2113/gsecongeo.74.2.260>
- 608 Hren, M., Tice, M. and Chamberlain, C., 2009. Oxygen and hydrogen isotope evidence
609 for a temperate climate 3.42 billion years ago. *Nature*, 462(7270): 205.
610 <https://doi.org/10.1038/nature08518>
- 611 Jaffrés, J. B., Shields, G. A. and Wallmann, K., 2007. The oxygen isotope evolution of
612 seawater: A critical review of a long-standing controversy and an improved

- 613 geological water cycle model for the past 3.4 billion years. *Earth-Science*
614 *Reviews*, 83(1-2), 83-122. <https://doi.org/10.1016/j.earscirev.2007.04.002>
- 615 Jaisi, D.P., Blake, R.E., 2014. Advances in using oxygen isotope ratios of phosphate
616 to understand phosphorus cycling in the environment.. In: *In Advances in*
617 *Agronomy*, 125. Academic Press, pp. 1–53.
- 618 Jallad, I. S., Abu Murry, O. S. and Sadaqah, R. M., 1989, Upper Cretaceous
619 phosphorites of Jordan, in: Notholt, A. J. G, Sheldon R. P. and Davidson, D. F.
620 (Eds.) *Phosphate Deposit of the World*, Vol. 2, *Phosphate Rock Resources*,
621 Cambridge Univ. Press, pp. 344-351.
- 622 Jarvis, I., 1995. Phosphorite geochemistry: state-of-the-art and environmental
623 concerns. *Oceanographic Literature Review*, 8: 639.
- 624 Kastner, M., Garrison, R., Kolodny, Y., Reimers, C. and Shemesh, A., 1990. Coupled
625 changes of oxygen isotopes in PO_4^{3-} and CO_3^{2+} in apatite, with emphasis on the
626 Monterey Formation, California. In: Riggs S.R., Burnett W.C. (Eds.), *Phosphate*
627 *Deposits of the World: Vol. 3, Genesis of Neogene to Modern Phosphorites*,
628 Cambridge Univ. Press, pp. 312-324
- 629 Klinkhammer, G.P. and Palmer, M.R., 1991. Uranium in the oceans: where it goes and
630 why. *Geochimica et Cosmochimica Acta*, 55(7), pp.1799-1806.
- 631 Khater, A.E.M., Galmed, M.A., Nasr, M.M. and El-Taher, A., 2016. Uranium and rare
632 earth elements in Hazm El-Jalamid phosphate, Saudi Arabia: concentrations and
633 geochemical patterns comparison. *Environmental Earth Sciences*, 75, 1261.
634 <https://doi.org/10.1007/s12665-016-6063-x>
- 635 Knauth, L. P. and Lowe, D. R., 2003. High Archean climatic temperature inferred from
636 oxygen isotope geochemistry of cherts in the 3.5 Ga Swaziland Supergroup,
637 South Africa. *Geological Society of America Bulletin*, 115(5), 566-580.
638 [https://doi.org/10.1130/0016-7606\(2003\)115<0566:HACTIF>2.0.CO;2](https://doi.org/10.1130/0016-7606(2003)115<0566:HACTIF>2.0.CO;2)

- 639 Knauth, L.P. and Epstein, S., 1976. Hydrogen and oxygen isotope ratios in nodular
640 and bedded cherts. *Geochimica et Cosmochimica Acta*, 40(9): 1095-1108.
641 [https://doi.org/10.1016/0016-7037\(76\)90051-X](https://doi.org/10.1016/0016-7037(76)90051-X)
- 642 Kolodny, Y. and Luz, B., 1992. Isotope signatures in phosphate deposits: Formation
643 and diagenetic history, Isotopic signatures and sedimentary records. In: Clauer
644 N., Chaudhuri S. (Eds.), *Lecture Notes in Earth Sciences*, Springer, pp. 69-121.
- 645 Kolodny, Y., and Kaplan, I.R., 1970. Uranium isotopes in sea-floor phosphorites.
646 *Geochimica et Cosmochimica Acta*, 34(1):3-24. [https://doi.org/10.1016/0016-7037\(70\)90148-1](https://doi.org/10.1016/0016-7037(70)90148-1)
- 648 Kusakabe, M. and Matsubaya, O., 1986. Volatiles in Magmas, volcanic gases, and
649 thermal waters. *Bull. Volcanol. Soc. Japan Spec. Issue* 30, 267-283 (in Japanese
650 with English abstract).
- 651 Land, L. S. and Lynch, F. L. (1996). $\delta^{18}\text{O}$ values of mudrocks: more evidence for an
652 ^{18}O -buffered ocean. *Geochimica et Cosmochimica Acta*, 60(17), 3347-3352.
653 [https://doi.org/10.1016/0016-7037\(96\)00185-8](https://doi.org/10.1016/0016-7037(96)00185-8)
- 654 Lecuyer, C., Grandjean, P. and Sheppard, S.M., 1999. Oxygen isotope exchange
655 between dissolved phosphate and water at temperatures $\leq 135\text{ }^{\circ}\text{C}$: inorganic
656 versus biological fractionations. *Geochimica et Cosmochimica Acta*, 63(6): 855-
657 862. [https://doi.org/10.1016/S0016-7037\(99\)00096-4](https://doi.org/10.1016/S0016-7037(99)00096-4)
- 658 Levina, S.D., Smilkstyn, A.O. and Karpov, L.N., Radioactivity of Phosphorites,
659 Litologiya fosforitonochnykh otlozhenii (Lithology of Phosphorite-Bearing
660 Sediments), In: Sokolova, A.S. (Eds), Moscow: Nauka, 1976, pp. 148–155.
- 661 Longinelli, A. and Nuti, S., 1968. Oxygen-isotope ratios in phosphate from fossil marine
662 organisms. *Science*, 160(3830): 879-882.
663 <https://doi.org/10.1126/science.160.3830.879>

- 664 Longinelli, A. and Nuti, S., 1973. Revised phosphate-water isotopic temperature scale.
- 665 Earth and Planetary Science Letters, 19(3): 373-376.
- 666 [https://doi.org/10.1016/0012-821X\(73\)90088-5](https://doi.org/10.1016/0012-821X(73)90088-5)
- 667 Lucas, J. and Abbas, M., 1989. Uranium in natural phosphorites: the Syrian example.
- 668 L'uranium dans les phosphorites naturelles: l'exemple syrien. Sciences
- 669 Géologiques, bulletins et mémoires, 42(3): 223-236. In: Lucas, J., Cook, J. P and
- 670 Prevot, L. (Eds.), Sciences Géologiques. Bulletin, tome 42, n°3, pp. 223-236.
- 671 <https://doi.org/10.3406/sgeol.1989.1824>
- 672 Makarov, E.A., 1963. Crystal chemistry of uranium minerals. In: Vinogradov, A.P.
- 673 (Eds.), Basic Features of Uranium Behaviour. Moscow, AN SSSR, pp. 27-45 (in
- 674 Russian).
- 675 McKelvey, V.E., 1967. Phosphate deposits, U.S. Geological Survey Bulletin, 1252-D,
- 676 pp. 1-22.
- 677 McManus, J., Berelson, W.M., Klinkhammer, G.P., Hammond, D.E. and Holm, C.,
- 678 2005. Authigenic uranium: relationship to oxygen penetration depth and organic
- 679 carbon rain. *Geochimica et Cosmochimica Acta*, 69(1): 95-108.
- 680 Menzel, R.G., 1968. Uranium, radium, and thorium content in phosphate rocks and
- 681 their possible radiation hazard. *Journal of Agricultural and Food Chemistry*, 16(2):
- 682 231-234.
- 683 Muehlenbachs, K., 1998. The oxygen isotopic composition of the oceans, sediments
- 684 and the seafloor. *Chemical Geology*, 145(3): 263-273.
- 685 [https://doi.org/10.1016/S0009-2541\(97\)00147-2](https://doi.org/10.1016/S0009-2541(97)00147-2)
- 686 Nathan, Y., 2012 Phosphate minerals. In: Nriagu JO, Moore PB (Eds.), Chapter 8, The
- 687 Mineralogy and Geochemistry of Phosphorites. Springer Science & Business
- 688 Media, ISBN: 978-3642617362

- 689 Notholt, A.J.G., 1986. Phosphate Deposits of the World: Volume 3, Neogene to Modern
690 Phosphorites, 156. Cambridge University Press.
- 691 Obersteiner, M., Peñuelas, J., Ciais, P., Van Der Velde, M. and Janssens, I.A., 2013.
692 The phosphorus trilemma. Nature Geoscience, 6(11): 897.
693 <https://doi.org/10.1038/ngeo1990>
- 694 Pantelica, A., Salagean, M., Georgescu, I. and Pincovschi, E., 1997. INAA of some
695 phosphates used in fertilizer industries. Journal of Radioanalytical and Nuclear
696 Chemistry, 216(2): 261-264. <https://doi.org/10.1007/BF02033788>
- 697 Parker, H. 1984. Tennessee Valley Authority National Fertilizer Development Center
698 progress 83 (No. TVA/OACD-84/4). Tennessee Valley Authority, Muscle Shoals,
699 AL (USA). Office of Agricultural and Chemical Development.
- 700 Partin, C. A., Bekker, A., Planavsky, N. J., Scott, C. T., Gill, B. C., Li, C. and Love, G.
701 D., 2013. Large-scale fluctuations in Precambrian atmospheric and oceanic
702 oxygen levels from the record of U in shales. Earth and Planetary Science Letters,
703 2013, 369: 284-293. <https://doi.org/10.1016/j.epsl.2013.03.031>
- 704 Petr P., 2016. Phosphate Rocks, Apatites and their Synthetic Analogues - Synthesis,
705 Structure, Properties and Applications, IntechOpen,
706 <https://doi.org/10.10.5772/62214>.
- 707 Piper, D.Z. and Kolodny, Y., 1987. The stable isotopic composition of a phosphorite
708 deposit: $\delta^{13}\text{C}$, $\delta^{34}\text{S}$, and $\delta^{18}\text{O}$. Deep Sea Research Part A. Oceanographic
709 Research Papers, 34(5-6), pp.897-911. [https://doi.org/10.1016/0198-0149\(87\)90044-6](https://doi.org/10.1016/0198-0149(87)90044-6)
- 711 Pokryshkin, V.I., 1981. Regularities of the Localization of Precambrian and
712 Phanerozoic Commercial-Grade Phosphorite Deposits in the World, Moscow:
713 Nedra.

- 714 Pufahl, P.K. and Groat, L.A., 2017. Sedimentary and Igneous Phosphate Deposits:
715 Formation and Exploration: An Invited Paper. *Economic Geology*, 112(3): 483-
716 516. <https://doi.org/10.2113/econgeo.112.3.483>
- 717 Robert, F. and Chaussidon, M., 2006. A palaeotemperature curve for the Precambrian
718 oceans based on silicon isotopes in cherts. *Nature*, 443(7114): 969.
719 <https://doi.org/10.1038/nature05239>
- 720 Rothbaum, H., McGaveston, D., Wall, T., Johnston, A. and Mattingly, G., 1979.
721 Uranium accumulation in soils from long-continued applications of
722 superphosphate. *Journal of Soil Science*, 30(1): 147-153.
723 <https://doi.org/10.1111/j.1365-2389.1979.tb00972.x>
- 724 Sattouf, M., 2007. Identifying the origin of rock phosphates and phosphorous
725 fertilizers using isotope ratio techniques and heavy metal patterns.
726 *Landbauforschung Völkenrode Special Issue 311*, Braunschweig.
- 727 Sattouf, M., Kratz, S., Diemer, K., Fleckenstein, J., Rienitz, D., Schiel, D. and Schnug,
728 E., 2008. Significance of uranium and strontium isotope ratios for retracing the
729 fate of uranium during the processing of phosphate fertilizers from rock
730 phosphates. In: De Kok, L.J. and Schnug, E. (Eds). *Loads and Fate of fertilizer-*
731 *derived uranium*. Backhuys Publishers, Leiden. pp: 978-90.
- 732 Sattouf, M., Kratz, S., Diemer, K., Rienitz, O., Fleckenstein, J., Schiel, D. and Schnug,
733 E., 2007. Identifying the origin of rock phosphates and phosphorus fertilizers
734 through high precision measurement of the strontium isotopes ^{87}Sr and ^{86}Sr .
735 *Landbauforschung Völkenrode*, 57: 01-11.
- 736 Schnug, E. and Haneklaus, N., 2015. Uranium in phosphate fertilizers—review and
737 outlook, In: Merkel B., Arab A. (Eds). *Uranium-Past and Future Challenges*.
738 Springer, pp. 123-130. https://doi.org/10.1007/978-3-319-11059-2_14

- 739 Schnug, E., Haneklaus, S., Schnier, C. and Scholten, L., 1996. Issues of natural
740 radioactivity in phosphates. Communications in Soil Science and Plant Analysis,
741 27(3-4): 829-841. <https://doi.org/10.1080/00103629609369600>
- 742 Shemesh, A., Kolodny, Y. and Luz, B., 1983. Oxygen isotope variations in phosphate
743 of biogenic apatites, II. Phosphorite rocks. Earth and Planetary Science Letters,
744 64(3): 405-416. [https://doi.org/10.1016/0012-821X\(83\)90101-2](https://doi.org/10.1016/0012-821X(83)90101-2)
- 745 Shemesh, A., Kolodny, Y. and Luz, B., 1988. Isotope geochemistry of oxygen and
746 carbon in phosphate and carbonate of phosphorite francolite. Geochimica et
747 Cosmochimica Acta, 52(11): 2565-2572. [https://doi.org/10.1016/0016-7037\(88\)90027-0](https://doi.org/10.1016/0016-7037(88)90027-0)
- 749 Shepherd, T.J., Rankin, A.H. and Alderton, D.H., 1985. A practical guide to fluid
750 inclusion studies. Blackie.
- 751 Sokolov, A. 1996. Evolution of the uranium potential of phosphorites. Geokhimiya,
752 1117-1119.
- 753 Soudry, D., Ehrlich, S., Yoffe, O. and Nathan, Y., 2002. Uranium oxidation state and
754 related variations in geochemistry of phosphorites from the Negev (southern
755 Israel). Chemical Geology, 189(3-4), pp.213-230.
- 756 Stephens, N.P. and Carroll, A.R., 1999. Salinity stratification in the Permian
757 Phosphoria sea; a proposed paleoceanographic model. Geology, 27(10): 899-
758 902. [https://doi.org/10.1130/0091-7613\(1999\)027<0899:SSITPP>2.3.CO;2](https://doi.org/10.1130/0091-7613(1999)027<0899:SSITPP>2.3.CO;2)
- 759 Syers, J.K., Mackay, A.D., Brown, M.W. and Currie, L.D., 1986. Chemical and physical
760 characteristics of phosphate rock materials of varying reactivity. Journal of the
761 Science of Food and Agriculture, 37(11): 1057-1064.
762 <https://doi.org/10.1002/jsfa.2740371102>
- 763 Tamburini, F., Bernasconi, S. M., Angert, A., Weiner, T. and Frossard, E. 2010. A
764 method for the analysis of the $\delta^{18}\text{O}$ of inorganic phosphate extracted from soils

- 765 with HCl. European Journal of Soil Science, 61(6), 1025-1032.
- 766 <https://doi.org/10.1111/j.1365-2389.2010.01290.x>
- 767 Tamburini, F., Pfahler, V., Büinemann, E.K., Guelland, K., Bernasconi, S.M. and
- 768 Frossard, E., 2012. Oxygen isotopes unravel the role of microorganisms in
- 769 phosphate cycling in soils. Environmental science & technology, 46(11): 5956-
- 770 5962. <https://doi.org/10.1021/es300311h>
- 771 Tang, C., Shindo, S. and Machida, I., 1998. Topographical effects on the distributions
- 772 of rainfall and ^{18}O distributions: a case in Miyake Island, Japan. Hydrological
- 773 processes, 12(4), 673-682. [https://doi.org/10.1002/\(SICI\)1099-1085\(19980330\)12:4<673::AID-HYP608>3.0.CO;2-Y](https://doi.org/10.1002/(SICI)1099-1085(19980330)12:4<673::AID-HYP608>3.0.CO;2-Y)
- 775 Taylor Jr, H. P. and Epstein, S., 1962. Relationship between $^{18}\text{O}/^{16}\text{O}$ ratios in
- 776 coexisting minerals of igneous and metamorphic rocks: part 1: principles and
- 777 experimental results. Geological Society of America Bulletin, 73(4), 461-
- 778 480.[https://doi.org/10.1130/0016-606\(1962\)73\[461:RBORIC\]2.0.CO;2](https://doi.org/10.1130/0016-606(1962)73[461:RBORIC]2.0.CO;2)
- 779 Taylor, H. P. 1968. The oxygen isotope geochemistry of igneous rocks. Contributions
- 780 to mineralogy and Petrology, 19(1), 1-71. <https://doi.org/10.1007/BF00371729>
- 781 U.S. Geological Survey, 2018, Mineral commodity summaries 2018: U.S. Geological
- 782 Survey, 200 p. <https://doi.org/10.3133/70194932>.
- 783 Van Kauwenbergh S. J., 2010. World phosphate rock reserves and resources. Muscle
- 784 Shoals, IFDC.
- 785 Van Kauwenbergh, S. J., 1997. Cadmium and other minor elements in world resources
- 786 of phosphate rock. Proceedings-Fertilizer Society No. 400, London.
- 787 Volkov, R., 1994. Geochemistry of uranium in Vendian-Cambrian phosphorites.
- 788 Geokhimiya, 7, 1042-1051.

- 789 Wakefield, Z. T., 1980. Distribution of cadmium and selected heavy metals in
790 phosphate fertilizer processing. National Fertilizer Development Center,
791 Tennessee Valley Authority.
- 792 Windmann, H., 2019. A contribution to the risk assessment of uranium contamination
793 in the food chain through phosphate containing fertilizers, feed and food
794 additives. PhD thesis, Faculty of Life Science, Technical University of
795 Braunschweig.
- 796 Zanin, Y. N., Zamirailova, A., Fomin, A., Gilinskaya, L. and Kireev, A., 2000. Uranium
797 of sedimentary apatite in catagenesis. *Geochemistry International*, 38, 452-458.
798 <https://doi.org/10.1134/S001670290701003X>
- 799 Zanin, Yu. N., Gilinskaya, L. G., Krasil'nikova, N. A., Krivoputskaya, L. M., Mirtov, Yu.
800 V. and Stolpovskaya, V. N., 1985. Calcium phosphates in phosphates of different
801 types. *International Geology Review*, 27(10): 1212-1229, <https://doi.org/10.1080/00206818509466496>
- 803
- 804
- 805
- 806
- 807
- 808
- 809
- 810
- 811
- 812
- 813
- 814

815 **Supplementary material**

816

817 **'Co-evolution' of Uranium Concentration and Oxygen Stable Isotope in
818 Phosphate Rocks**

819 Y.Sun^{1,2*}, W. Amelung^{1,2}, B. Wu¹, S. Haneklaus³, M. Maekawa³, A. Lücke¹, E. Schnug³,
820 R. Bol¹

821 ¹Institute of Bio- and Geosciences: Agrosphere (IBG-3), Forschungszentrum Jülich
822 GmbH, 52425 Jülich, Germany

823 ²University of Bonn, Institute of Crop Science and Resource Conservation, Soil
824 Science and Soil Ecology, Nussallee 13, 53115 Bonn, Germany.

825 ³ Institute for Crop and Soil Science, Julius Kühn-Institut, Federal Research Institute
826 for Cultivated Plants, Bundesallee 69, 38640 Braunschweig, Germany

827

828 * Corresponding author (yajie.sun@uni-bonn.de)

829

830

831

832

833

Table S1. Literature review and own data on uranium concentrations in phosphate rocks

Country	Deposit	Type	Age	U ppm	P ₂ O ₅ %	U/P ₂ O ₅	Reference
Algeria	Djebel Onk	Phosphatic limestone; pelletal; granular;	Late Paleocene	31.0	32.4	1.0	Cevik et al., 2010
Algeria	Djebel Onk	Phosphatic limestone; pelletal; granular;	Late Paleocene	25.0	28.0	0.9	Khater et al., 2016
Algeria	Djebel Kouif	-	-	100.0	27.9	3.6	Parker, 1984
Algeria	Gebel Onk	Granular	Paleocene	8-115, 60	22-30, 21	2.8	Pokryshkin, 1981
Algeria	-	Rock phosphate	-	51.8	28.6	1.8	this study
Algeria	-	Rock phosphate	-	52.7	28.8	1.8	this study
Algeria	-	Rock phosphate	-	53.3	28.7	1.9	this study
Algeria	-	Rock phosphate	-	53.5	28.6	1.9	this study
Algeria	-	Calcined phosphate	-	59.9	31.1	1.9	this study
Algeria	-	Rock phosphate	Cretaceous-Eocene	45.0	25.9	1.7	this study
Algeria	-	Rock phosphate	-	47.8	29.7	1.6	this study
Algeria	-	Rock phosphate	-	48.6	30.0	1.6	this study
Algeria	Djebel Onk	Phosphatic limestone; pelletal; granular;	Late Paleocene	25.0	29.3	0.9	Van Kauwenbergh, 1997
Antarctica	Pensacola	Nodules, matrix	Devonian	260.0	30.0	8.6	Altschuler, 1980
Australia	Eastern slope	Nodules	Middle Miocene-Early Pliocene	27-303, 126	11.0	11.9	Cook et al., 1990
Australia	Eastern slope	Nodules	Middle Miocene-Early Pliocene	67.0	9.6	3-13.7.9	Cook et al., 1990
Australia	North Queensland	Argillite-type phosphorites	Early-Middle Cambrian	15-65, 48	7.8-39.1, 18.6	2.6	Cook, 1972
Australia	North Queensland	Replacement phosphorites	Early-Middle Cambrian	10-80, 43	28-39.2, 35.3	1.2	Cook, 1972

Australia	North Queensland	Pelletal phosphorites	Early-Middle Cambrian	45-130, 78	33.7-37.4, 35.6	2.2	Cook, 1972
Australia	Wonarah	Leached phosphorites	Early-Middle Cambrian	2-53, 21.9	17.3-30.9, 24.7	0.1-2.3, 0.9	Howard and Hough, 1979
Australia	D Tree	Leached	Early-Middle Cambrian	8-74, 23	14.4-27.9, 21.7	0.4-3.7, 1.1	Howard and Hough, 1979
Australia	D Tree	Replacement phosphorites	Early-Middle Cambrian	18-45, 33	37.6-39.5, 38.7	0.5-1.2, 0.9	Howard and Hough, 1979
Australia	Sherrin Creek (Queensland)	Unleached phosphorites	Early-Middle Cambrian	5-42, 25	28-37.8, 25	0.6-4.3, 1.2	Howard and Hough, 1979
Australia	D Tree	Partly leached	Early-Middle Cambrian	19-86, 47	7.8-27.4, 19.9	1-5.2, 2.5	Howard and Hough, 1979
Australia	D Tree	Unleached phosphorites	Early-Middle Cambrian	19-61, 32	3.8-15.5, 8.6	3.1-5.6, 3.9	Howard and Hough, 1979
Australia	Duchess	-	Early Middle Cambrian	80.0	29.1	2.7	Parker, 1984
Australia	Duchess	-	Early Middle Cambrian	80.0	23.9	3.3	Parker, 1984
Australia	Duchess	-	Early Middle Cambrian	92.0	31.2	2.9	Van Kauwenbergh, 1997
Azerbaijan	-	shelly	Ordovician	35-52, 43	5.7-14.4, 10	2.4-9.1, 5.6	Baturin and Kochenov, 2001
Brazil	Bambui	pelletal	Precambrian	30.0	19-35.27	1-1.5, 1.2	Altschuler, 1980
Brazil	-	Rock phosphate	Middle-Late Proterozoic	38.1	28.6	1.3	this study
Brazil	-	Rock phosphate	Middle-Late Proterozoic	67.5	25.0	2.7	this study
Burkina Faso	Kodjari	-	Middle-Late Proterozoic	125.0	25.4	4.9	Van Kauwenbergh, 1997
China	Wanjhawan	Vaguely granular	Early-Middle Cambrian	12.9	26.0	0.5	Volkov, 1994
China	Kunjian	Granular	Early-Middle Cambrian	15.8	31.0	0.5	Volkov, 1994
China	Undifferentiated	-	-	10.0	31.9	0.3	Parker, 1984
China	Undifferentiated	-	-	-	20.0	30.3	Parker, 1984
China	Hubei, Jingzhou	Sedimentary type	Late Proterozoic	2.0	22.2	0.1	this study

China	Hubei, Jingzhou	Sedimentary type	Late Proterozoic	2.6	30.7	0.1	this study
China	Hunan, Shimen	Metamorphic type	Late Proterozoic	3.0	25.0	0.1	this study
China	Hubei, Yichang	Sedimentary type	Late Proterozoic	3.0	22.2	0.2	this study
China	Hubei, Jingmen	Sedimentary type	Late Proterozoic	3.7	29.8	0.2	this study
China	Hubei, Yichang	Sedimentary type	Late Proterozoic	5.0	25.2	0.2	this study
China	Hubei, Yichang	Sedimentary type	Late Proterozoic	5.6	31.4	0.2	this study
China	Hubei, Yichang	Sedimentary type	Late Proterozoic	7.2	30.9	0.4	this study
China	Guizhou, Kaiyang	Sedimentary type	Late Proterozoic	11.4	28.9	0.7	this study
China	Sichuan, Shijiao	Sedimentary type	Middle-Late Devonian	19.5	29.8	0.5	this study
China	Yunnan, Kunming	Sedimentary type	Early Cambrian	14.7	23.8	0.6	this study
China	Sichuan, Hanyuan	Sedimentary type	Middle-Late Devonian	14.3	23.6	1.0	this study
China	Yunnan, Kunming	Sedimentary type	Early Cambrian	22.6	27.0	0.8	this study
China	Yunnan, Jinning	Sedimentary type	Early Cambrian	20.4	21.1	1.5	this study
China	Kaiyang	Sedimentary type	Late Proterozoic	31.0	35.9	0.9	Van Kauwenbergh, 1997
Egypt	East Sabaiya	-	Late Cretaceous	57.0	30.6	1.9	Cevik et al., 2010
Egypt	Kosseir	-	Late Cretaceous	40.0	28.3	1.4	Parker, 1984
Egypt	Abu Tartur	Bedded	Late Cretaceous	40.0	26.5	1.5	Parker, 1984
Egypt	Safaga	Granular	Late Cretaceous	100.0	28.9	3.5	Parker, 1984
Egypt	Safaga	Bedded; pelletal;	Late Cretaceous	130.0	32.2	4.0	Parker, 1984
Egypt	Safaga	Bedded; pelletal;	Late Cretaceous	130.0	31.8	4.1	Parker, 1984
Egypt	Safaga	Granular	Late Cretaceous	70-120,95	25.0	3-5, 4	Sokolov, 1996

Egypt	Abu Tartur	Bedded	Late Cretaceous	120.0	31.7	3.8	Van Kauwenbergh, 1997
Egypt	West Makamid	-	-	100.0	26.5	3.8	Van Kauwenbergh, 1997
Egypt	Hamrawen	-	Late Cretaceous	110.0	22.2	5.0	Van Kauwenbergh, 1997
Estonia	Toolse	Shelly	Ordovician	15-45, 30	6.5-8.7, 7.6	2.3-5.2, 3.7	Baturin and Kochenov, 2001
Estonia	Narva	Shelly	Ordovician	52-100, 76	6.4-7.1, 6.8	7.3-15.5, 9.4	Baturin and Kochenov, 2001
Estonia	Toolse	Shelly	Ordovician	34.0	11.5	2.9	Levina et al., 1976
Egypt	EI-Sibayia	Bedded	Late Cretaceous	89.0	30.0	3.0	Khater et al., 2016
Egypt	EI-Sibayia	Bedded	Late Cretaceous	89.0	27.0	3.3	Khater et al., 2016
India	Hirapur	stromatolitic	Proterozoic	3-120,			Banerjee et al., 1982
India	Uttar Pradesh	Granular	Proterozoic	1.7-129.7	28.8-31.8	0.05-4.23	Dar et al., 2014
India	Rajasthan	Stromatolitic	Early Proterozoic	20.0	40.1	0.5	Parker, 1984
India	Udaipur	stromatolitic	Proterozoic	30-100, 65	10-37, 23	2.8	Pokryshkin, 1981
India	Mussoorie	-	Early Cambrian	26.0	25.0	1.0	Van Kauwenbergh, 1997
India	Aravalli	Stromatolitic	Proterozoic	3.6-4.2, 4	31.7-33.1, 32.4	0.1	Zanin et al. 2000
India	Aravallian basin	Stromatolitic	Proterozoic	3.6	31.7	0.1	Zanin et al. 2000
India	Aravallian basin	Stromatolitic	Proterozoic	4.2	33.1	0.1	Zanin et al. 2000
Israel	Mishash	Granular	Late Cretaceous-Paleocene	105.0	22-33,27.5	3.3	Makarov, 1963
Israel	Arad	granular, pellets	Late Cretaceous	150.0	32.3	4.6	Parker, 1984
Israel	-	-	Paleogene	40-240,140	16-27,22	6.3	Pokryshkin, 1981
Israel	Oron	Granular	Late Cretaceous	8-115, 60	20-32, 26	2.3	Pokryshkin, 1981

Israel	Arad	granular, pellets	Late Cretaceous	153.0	32.1	4.8	Syers et al., 1986
Israel	Arad	Rock phosphate	Late Cretaceous	153.0	33.0	4.6	this study
Israel	Arad	Rock phosphate	Late Cretaceous	148.0	32.9	4.5	this study
Israel	-	Rock phosphate	-	128.0	33.9	3.8	this study
Israel	-	Rock phosphate	-	127.4	33.3	3.8	this study
Israel	-	Rock phosphate	-	125.0	33.1	3.8	this study
Israel	-	Rock phosphate	-	152.0	32.4	4.7	this study
Israel	-	Rock phosphate	-	111.0	26.8	4.1	Van Kauwenbergh, 1997
Israel	Oron	Granular	Late Cretaceous	99.0	33.6	2.9	Van Kauwenbergh, 1997
Israel	Arad	granular, pellets	Late Cretaceous	148.0	32.8	4.5	Van Kauwenbergh, 1997
Israel	Nahal Zin	Rock phosphate	Late Cretaceous	129.0	38.0	3.4	this study
Israel	Oron	Rock phosphate	Late Cretaceous	215.0	33.9	6.3	this study
Japan	submarine rise of the sea of Japan	Granular	Miocene	12-110, 50	10.5-32.3, 21.4	0.4-5,2.7	Baturin and Kochenov, 2001
Jordan	-	Granular	Late Cretaceous-Paleocene	67-155, 111	20-34, 27	4.1	Volkov, 1994
Jordan	El Hassa	Granular	Late Cretaceous-Maastrichtian	82.0	32.5	2.5	Jallad et al., 1989
Jordan	El Hassa	Granular	Late Cretaceous Maastrichtian	105.0	33.9	3.1	Jallad et al., 1989
Jordan	-	Granular	Late Cretaceous-Paleocene	90-180,135	20-34,27	5.0	Nabil, 1992
Jordan	Ruseifa	Granular	Late Cretaceous	129.0	30.8	4.2	Parker, 1984

Jordan	El Hassa	Granular	Late Cretaceous Maastrichtian	8-180, 94	23-34,28	3.3	Pokryshkin, 1981
Jordan	El Hassa	Granular	Late Cretaceous Maastrichtian	72.0	30.7	2.3	Syers et al., 1986
Jordan	Shidyia	granular	Late Cretaceous	46.0	30.5	1.5	Van Kauwenbergh, 1997
Jordan	El Hassa	Granular	Late Cretaceous	54.0	31.7	1.7	Van Kauwenbergh, 1997
Kazakhstan	Chilisai	Nodules	Eocene	16-53, 29	6.4-13.3, 9.8	2.9	Levina et al., 1976
Kazakhstan	Kara Tau	Bedded (microcrystalline)	Lower Cambrian	22.7	18.6	1.2	Zanin et al. 2000
Kazakhstan	Kara Tau	Bedded (microcrystalline)	Lower Cambrian	25.0	16.1	1.6	Zanin et al. 2000
Mali	Tilemsi	Nodules	Middle Eocene	123.0	28.8	4.3	Van Kauwenbergh, 1997
Mongolia	Hubsugul	Granular and structureless	Early Cambrian	1-31, 11	16-37, 20.7	0.5	Levina et al., 1976
Morocco	Ypusoufia	-	Late Cretaceous-Early Eocene	83.0	30.0	2.8	Cevik et al., 2010
Morocco	-	Granular	Late Cretaceous-Eocene	140.0	33.0	4.2	Altschuler, 1980
Morocco	-	-	-	140.0	33.0	4.2	Altschuler, 1980
Morocco	Khouribge	Bedded	Late Cretaceous-Early Eocene	88.0	33.0	2.7	Khater et al., 2016
Morocco	Youssoufia	Bedded	Late Cretaceous-Early Eocene	97.0	31.0	3.1	Khater et al., 2016
Morocco	Bu Craa	Bedded	Late Cretaceous-Paleocene	70.0	35.3	2.0	Parker, 1984
Morocco	Bu Craa	Bedded	Late Cretaceous-Paleocene	80.0	34.9	2.3	Parker, 1984

Morocco	-	-	-	120.0	31.8	3.8	Parker, 1984
Morocco	-	-	-	130.0	32.2	4.0	Parker, 1984
Morocco	-	Granular	Late Cretaceous-Eocene	57-190, 120	15-33, 24	5.0	Pokryshkin, 1981
Morocco	-	Rock phosphate	-	112.0	31.0	3.6	this study
Morocco	-	Rock phosphate	-	191.0	30.2	6.3	this study
Morocco	-	Rock phosphate	-	127.4	30.8	4.1	this study
Morocco	-	Rock phosphate	-	147.0	34.4	4.3	this study
Morocco	Khouribga	Rock phosphate	Late Cretaceous-Middle Eocene	127.5	31.4	4.1	this study
Morocco	Khouribga	Rock phosphate	Late Cretaceous-Middle Eocene	128.0	31.9	4.0	this study
Morocco	Khouribga	Rock phosphate	Late Cretaceous-Middle Eocene	245.0	34.4	7.1	this study
Morocco	Khouribga	Bedded; granular; shell	Late Cretaceous-Middle Eocene	81.0	32.3	2.5	Van Kauwenbergh, 1997
Morocco	Khouribga	Bedded; granular; shell	Late Cretaceous-Middle Eocene	100.0	33.4	3.0	Van Kauwenbergh, 1997
Morocco	Youssoufia	Bedded	Late Cretaceous-Early Eocene	111.0	32.5	3.4	Van Kauwenbergh, 1997
Morocco	Khouribga	Bedded; granular; shell	Late Cretaceous-Middle Eocene	82.0	33.4	2.5	Van Kauwenbergh, 1997
Morocco	Youssoufia	Bedded	Late Cretaceous-Early Eocene	97.0	32.1	3.0	Van Kauwenbergh, 1997

Morocco	Youssoufia	Bedded	Late Cretaceous-Early Eocene	89.0	27.6	3.2	Van Kauwenbergh, 1997
Nauru	-	-	-	40.0	37.1	1.1	Parker, 1984
Nauru	-	-	-	50.0	38.5	1.3	Parker, 1984
Nauru	-	-	-	60.0	38.7	1.6	Parker, 1984
Nauru	-	-	-	64.0	35.7	1.8	Syers et al., 1986 Kolodny and Kaplan, 1970
New Zealand	submarine bChatham rise	Granular	Miocene	117-524, 230	21.8	5-24,14	
Niger	Tapoa	Granular	Early Cambrian	7.1	27.0	0.3	Volkov, 1994
Niger	Tapoa	Granular	Late Proterozoic	8.2	31.0	0.3	Volkov, 1994
Niger	Parc W	-		65.0	33.5	1.9	Van Kauwenbergh, 1997
Peru	Peru shelf	Curst	Pleistocene-Holocene	12-38, 23	2.1-9.4, 4.4	3-8,3.5	Baturin and Kochenov, 2001
Peru	Peru shelf	Curst	Pleistocene-Holocene	52-193, 106	11.2-25.2, 14.7	4.6- 8.3,4.9	Baturin and Kochenov, 2001
Peru	Peru shelf	Nodular	Pleistocene-Holocene	16-182, 93	5.9-28.7, 17.3	2.0- 17.7,5.3	Burnett and Veeh, 1977
Peru	Sechura	Pelletal	Middle Miocene	72.0	29.5	2.4	Parker, 1984
Peru	Sechura	Pelletal	Middle Miocene	80.0	30.8	2.6	Parker, 1984
Peru	Sechura	Pelletal	Middle Miocene	80.0	29.7	2.7	Parker, 1984
Peru	Sechura	Pelletal	Middle Miocene	47.0	29.3	1.6	Van Kauwenbergh, 1997
Peru	Sechura	Pelletal	Middle Miocene	80.0	31.3	2.6	Van Kauwenbergh, 1997
Portugal	Continental slope	Nodular	Miocene	5-158, 80	6.4-21.5, 14	0.5- 11.1,5.5	Gaspar, 1981
Russia	Seleuk	Nodules	Late Jurassic-Paleogene	4.2	13.5	0.3	Baturin and Kochenov, 2001
Russia	Egor'ev	Nodular	Late Jurassic-early Cretaceous	17.0	12.6	1.3	Baturin and Kochenov, 2001

Russia	Penze	Nodules	Late Jurassic-Paleogene	31.0	24.1	1.3	Baturin and Kochenov, 2001
Russia	Bessonov	Nodules	Late Jurassic-Paleogene	27.0	19.2	1.4	Baturin and Kochenov, 2001
Russia	Bogdanov	Nodules	Late Jurassic-Paleogene	27.0	18.4	1.5	Baturin and Kochenov, 2001
Russia	Trukhanov	Nodules	Late Jurassic-Paleogene	27.0	17.9	1.5	Baturin and Kochenov, 2001
Russia	Tarkhanov	Nodules	Late Jurassic-Paleogene	31.0	20.1	1.5	Baturin and Kochenov, 2001
Russia	Tambov	Nodules	Late Jurassic-Paleogene	45.0	24.9	1.8	Baturin and Kochenov, 2001
Russia	Kingisepp, Baltic region	Shelly	Ordovician	24.0	12.5	2.0	Baturin and Kochenov, 2001
Russia	Egor'ev	Nodular	Late Jurassic-early Cretaceous	50.0	23.3	2.1	Baturin and Kochenov, 2001
Russia	Podbuga	Nodules	Late Jurassic-Paleogene	45.0	18.3	2.5	Baturin and Kochenov, 2001
Russia	Krolevitskoe	Nodules	Late Jurassic-Paleogene	40.0	16.1	2.5	Baturin and Kochenov, 2001
Russia	Undor	Nodules	Late Jurassic-Paleogene	59.0	23.2	2.5	Baturin and Kochenov, 2001
Russia	Oraush	Nodules	Late Jurassic-Paleogene	68.0	25.3	2.7	Baturin and Kochenov, 2001
Russia	Polpino	Nodules	Late Cretaceous	52.0	16.1	3.2	Baturin and Kochenov, 2001
Russia	Shchigrov	Nodules	Late Jurassic-Paleogene	68.0	16.0	4.3	Baturin and Kochenov, 2001
Russia	Slobodsk-Kostoretsk	Nodules	Late Jurassic-Paleogene	40.0	6.9	5.8	Baturin and Kochenov, 2001
Russia	Trekhostrovsk	Nodules	Late Jurassic-Paleogene	88.5	12.6	7.0	Baturin and Kochenov, 2001
Russia	Vyatka-Kama	Shelly	Late Jurassic-Paleogene	17-59, 38	12.6-23.3, 18.0	0.7-4.6, 2.6	Baturin and Kochenov, 2001
Russia	Maardu, ibidem	Shelly	Ordovician	14-68, 41	10.8-26, 18	1.3-2.6, 2.0	Baturin and Kochenov, 2001
Russia	Maardu, ibidem	Shelly conglomerate	Ordovician	24.0	17.0	1.4	Levina et al., 1976

Russia	Maardu, ibidem	shelly	Ordovician	7-48, 21	3.0-29, 13	1.6	Levina et al., 1976
Russia	Egor'ev	Nodular	Late Jurassic-early Cretaceous	34.0	21.1	1.6	Levina et al., 1976
Russia	Egor'ev	Phosphatized fauna	Late Jurassic-early Cretaceous	40.0	32.1	1.7	Levina et al., 1976
Russia	Vyatka-Kama	Phosphatized fauna	Late Jurassic-Paleogene	40.0	23.1	1.7	Levina et al., 1976
Russia	Gornaya shoria	Brecciated	Late Proterozoic	10-60, 35	5-13.6, 12	2.4	Levina et al., 1976
Russia	Maardu, ibidem	Phosphatized sandstone	Ordovician	20.0	8.2	2.4	Levina et al., 1976
Russia	Lagap(Shantar Island)	Brecciated	Early-Middle Cambrian	7-56, 25	5-32, 20	2.5	Levina et al., 1976
Russia	Vyatka-Kama	Nodules	Late Jurassic-Paleogene	17-58, 34	10.7-19.5, 12.2	2.8	Levina et al., 1976
Russia	Maardu, ibidem	Pebble	Ordovician	25.0	8.6	2.9	Levina et al., 1976
Russia	Polpino	Nodules	Late Cretaceous	1-111, 43	5-8, 7	2-12, 4.8	Levina et al., 1976
Russia	Polpinsk	Nodular	Upper Cretaceous	30.4	27.8	1.1	Zanin et al. 2000
Russia	Egor'ev	Nodular	Upper Jurassic-lower Cretaceous	29.6	25.8	1.1	Zanin et al. 2000
Russia	Egor'ev	Nodular	Upper Jurassic-lower Cretaceous	29.6	25.8	1.1	Zanin et al. 2000
Russia	Egor'ev	Nodular	Upper Jurassic-lower Cretaceous	30.7	25.5	1.2	Zanin et al. 2000
Russia	Polpinsk	phosphatic wood	Upper Cretaceous	55.8	28.5	2.0	Zanin et al. 2000
Russia	Egor'ev	Nodular	Upper Jurassic-lower Cretaceous	35.2	15.8	2.2	Zanin et al. 2000
Russia	Polpinsk	phosphatic wood	Upper Cretaceous	66.5	28.8	2.3	Zanin et al. 2000

Russia	Polpinsk	Upper phosphatic wood	Upper Cretaceous	100.0	20.8	4.8	Zanin et al. 2000
Russia	Sakhalin Island	Nodular	Neogene	8.2	15.5	0.5	Zanin et al. 2000
Russia	Sakhalin Island	Nodular	Neogene	17.9	26.8	0.7	Zanin et al. 2000
Saudi Arabia	Al-Jalamid	bedded; pelletal	Early Paleocene	21.0	21.0	1.0	Khater et al., 2016
Saudi Arabia	Al-Jalamid	bedded; pelletal	Early Paleocene	21.0	21.0	1.0	Khater et al., 2016
Saudi Arabia	Amm Wa ual	bedded; pelletal	Paleocene-Oligocene	61.0	32.0	1.9	Khater et al., 2016
Saudi Arabia	Amm Wa ual	bedded; pelletal	Paleocene-Oligocene	62.0	27.0	2.3	Khater et al., 2016
Saudi arabia	-	Granular	Late Cretaceous-Paleocene	16-90, 53	18.1-31.4, 24.7	2.1	Pokryshkin, 1981
Seamounts of the Pacific Ocean	-	Phosphatized limestones, breccia, and effusives	Late Cretaceous-Quaternary	1.3-9.2	4.8-31.6	0.06-0.7	Baturin et al., 1982
Senegal	Taiba	Bedded	Middle Eocene-Oligocene	67.0	36.0	1.9	Khater et al., 2016
Senegal	Taiba	Rock phosphate	Middle Eocene-Oligocene	96.0	36.7	2.6	this study
Senegal	Taiba	Rock phosphate	Middle Eocene-Oligocene	90.0	36.6	2.5	this study
Senegal	Taiba	Granular	Middle Eocene-Oligocene	70.0	27.2	2.6	Parker, 1984
Senegal	Taiba	Granular	Middle Eocene-Oligocene	100-150,125	25-31, 29	2.6	Pokryshkin, 1981
Senegal	Taiba	Granular	Middle Eocene-Oligocene	64.0	36.9	1.7	Van Kauwenbergh, 1997
Senegal	Taiba	Granular	Middle Eocene-Oligocene	99.0	37.0	2.6	Zanin et al. 2000
Senegal	Taiba	Granular	Middle Eocene-Oligocene	154.0	38.0	4.1	Zanin et al. 2000
Siberia	Siberian platform, Vikhoreva river	Shelly	Middle Ordovician	11.0	38.2	0.3	Zanin et al. 2000

area, Angara River Basin	Siberia	Middle Ordovician	11.0	37.2	0.3	Zanin et al. 2000	
Siberian platform, Vikhoreva river area, Angara River Basin	Siberia	Shelly					
Siberian platform, Kuonamka Formation, Kachelkuan River valley	Siberia	Nodular					
Siberian platform, Kuonamka Formation, Kachelkuan River valley	Siberia	Nodular					
South Africa	Southern of African	Upper Lower Cambrain	56.6	29.0	2.0	Zanin et al. 2000	
Syria	Hims-Palmyra (Aisharqa)	Upper Lower Cambrain	374.2	26.1	14.3	Zanin et al. 2000	
Syria	-	Upper Lower Cambrain	11.2	38.0	0.3	this study	
Syria	-	Upper Lower Cambrain	10-166, 79	17.3-24, 21	0.4-9.8, 5.1	Kolodny and Kaplan, 1970	
Syria	-	Upper Lower Cambrain	120-140, 130	25.0	4-6, 5	Volkov, 1994	
Syria	-	Upper Lower Cambrain	30-200, 115	25.0	4.6	Baturin and Kochenov, 2001	
Syria	-	Upper Lower Cambrain	36.0	26.7	1.4	Cevik et al., 2010	
Syria	-	Upper Lower Cambrain	20-319, 82	18-36, 26.3	3.2	Lucas and Abbas, 1989	
Syria	-	Rock phosphate	-	58.6	24.6	2.4	this study
Syria	-	Rock phosphate	-	58.6	24.6	2.4	this study
Syria	Khneifies	Rock phosphate bedded	Late Cretaceous	75.0	31.9	2.4	Van Kauwenbergh, 1997
Syria	Khneifies	Ground rock phosphate	Late Cretaceous	59.5	30.4	2.0	this study

Syria	Ain Layloun	Friable phosphate rock	Cretaceous	31.2	4.4	this study
Tanzania	Minjingu	-	Neogene-Quaternary	28.6	13.6	Van Kauwenbergh, 1997
Togo	-	Rock phosphate	Middle Eocene	36.7	3.0	Parker, 1984
Togo	-	Rock phosphate	Early-Middle Eocene	107.0	2.9	this study
Togo	-	Rock phosphate	Early-Middle Eocene	104.0	33.7	this study
Togo	-	Rock phosphate	-	96.7	36.0	this study
Togo	-	-	-	77.0	36.5	Van Kauwenbergh, 1997
Togo	-	-	Early-Middle Eocene	93.0	37.0	Khater et al., 2016
Tunisia	Gafsa	-	Paleocene-Early Eocene	20.0	26.1	Cevik et al., 2010
Tunisia	-	-	-	44.0	29.0	Khater et al., 2016
Tunisia	-	-	Paleocene-Early Eocene	12.0	29.2	Parker, 1984
Tunisia	-	-	Paleocene-Early Eocene	30.0	29.5	Parker, 1984
Tunisia	-	-	Paleocene-Early Eocene	40.0	29.2	Parker, 1984
Tunisia	-	-	Paleocene-Early Eocene	50.0	28.0	Parker, 1984
Tunisia	-	-	Paleocene-Early Eocene	88.0	30.7	Parker, 1984
Tunisia	Gafsa	Granular	Paleogene	35-75, 55	25-31, 28	Pokryshkin, 1981
Turkey	Mardin	Granular	Late Cretaceous-Paleocene	25-57, 40	10-25, 17.5	Baturin and Kochenov, 2001
Turkey	Mazidagi	bedded; pelletal; nodular; oolitic; fossiliferous (fish remains and bones); limonitic and glauconitic phosphatic limestone	Late Cretaceous	33.0	33.5	Cevik et al., 2010
Ukraine	Podol region	Concretionary radiated	Vendian	0.6	24.8	Zanin et al. 2000

Ukraine	Podol region	Concretionary radiated	Vendian	0.9	35.3	0.0
Ukraine	Podol region	Concretionary radiated	Vendian	3.4	33.0	0.1
Ukraine	Podol region	Concretionary radiated	Vendian	4.2	35.1	0.1
USA	Continental slope of Carolina	Nodular	Miocene	40-130, 77	22.4-29.7, 26	1.4- 5.8,3.6
USA	Pango River, North Carolina	Granular	Miocene	65.0	30.0	2.0
USA	Bone Valley, Florida	Granular and nodular	Miocene-Pliocene	140.0	30-35, 33	4.4
USA	Phosphoria	Microgranular	Permian	20-210, 90	23-37, 30	3.0
USA	North Florida	-	Middle-Late Permian	81.0	31.0	2.6
USA	Idaho	-	Early-Middle Miocene	107.0	32.0	3.3
USA	Florida	-	Miocene	141.0	32.0	4.4
USA	submarine Blake plateau	Nodular	Miocene	18-70, 37	18-20, 19	1-4,2.5
USA	North Florida	-	Miocene-Pliocene	50.0	30.9	1.6
USA	North Carolina	bedded; granular	Early-Middle Miocene	60.0	30.5	2.0
USA	North Florida	-	Miocene-Pliocene	70.0	32.5	2.2
USA	Idaho	peloidal	Middle-Late Permian (late paleozoic)	70.0	32.3	2.2
USA	North Carolina	bedded; granular	Early-Middle Miocene	70.0	30.0	2.3
USA	North Carolina	bedded; granular	Early-Middle Miocene	93.0	30.2	3.1
USA	Idaho	peloidal	Middle-Late Permian (late paleozoic)	110.0	32.0	3.4

USA	Idaho	peloidal	Middle-Late Permian (late paleozoic)	110.0	30.2	3.6	Parker, 1984
USA	Central Florida	-	Neogene	120.0	32.2	3.7	Parker, 1984
USA	Central Florida	-	Neogene	160.0	32.7	4.9	Parker, 1984
USA	Central Florida	-	Neogene	150.0	27.8	5.4	Parker, 1984
USA	Central Florida	-	Neogene	200.0	30.7	6.5	Parker, 1984
USA	Lower Carolina	Nodular	Neogene	3-65, 30	8.5-21, 15	2.0	Pokryshkin, 1981
USA	Hawthorne Formation, Florida	Granular and nodular	Miocene	40-65, 50	10-25, 17	3.0	Pokryshkin, 1981
USA	North Carolina	Granular	Miocene	25-250, 135	11-18, 15	9.0	Pokryshkin, 1981
USA	North Carolina	bedded; granular	Early-Middle Miocene Miocene- Pliocene	65.0	29.1	2.2	Syers et al., 1986
USA	North Florida	-	143.0	30.5	4.7	Syers et al., 1986	
USA	Florida	Rock phosphate	-	74.0	32.1	2.3	this study
USA	North Florida	Pebble phosphate	-	103.0	31.1	3.3	this study
USA	North Florida	Rock phosphate	Early-Middle Miocene; Holocene	104.0	33.5	3.1	this study
USA	South Florida	Pebble phosphate	-	128.0	36.0	3.6	this study
USA	Florida	Pebble phosphate	-	114.0	32.4	3.5	this study
USA	Florida	Pebble phosphate	-	112.0	34.3	3.3	this study
USA	Florida	Rock phosphate	late Miocene	95.3	31.4	3.0	this study
USA	Florida	Rohphosphat normal (Pebble- Phosphat)	Early-Middle Miocene	154.0	32.6	4.7	this study
USA	Pebble phosphate, commercial quality	-	-	153.0	30.4	5.0	this study
USA	Pebble phosphate	-	-	104.2	32.4	3.2	this study

USA	Florida	Rohphosphat Pebble	Early-Middle Miocene	147.0	28.4	5.2	this study
USA	Florida	Rock phosphate (as raw material)	Early-Middle Miocene	191.0	33.3	5.7	this study
USA	Central Florida	-	Neogene	128.4	34.6	3.7	Van Kauwenbergh, 1997
USA	Idaho	peloidal	Middle-Late Permian (late paleozoic)	141.0	30.2	4.7	Van Kauwenbergh, 1997
USA	Central Florida	-	Neogene	135.0	33.3	4.0	Van Kauwenbergh, 1997
USA	North Carolina	bedded; granular	Early-Middle Miocene	41.0	29.9	1.4	Van Kauwenbergh, 1997
USA	Idaho	peloidal	Middle-Late Permian (late paleozoic)	60.0	32.6	1.8	Van Kauwenbergh, 1997
USA	Central Florida	-	Neogene	59.0	31.0	1.9	Van Kauwenbergh, 1997
USA	North Carolina	bedded; granular	Early-Middle Miocene	70.0	32.2	2.2	Van Kauwenbergh, 1997
USA	Central Florida	-	Neogene	128.5	34.5	3.7	Van Kauwenbergh, 1997
USA	North Carolina	bedded; granular	Early-Middle Miocene	58.0	28.1	2.1	Wakefield, 1980
USA	North Florida	-	Miocene-Pliocene	69.0	32.7	2.1	Wakefield, 1980
USA	North Carolina	bedded; granular	Miocene-Pliocene	66.0	31.1	2.1	Wakefield, 1980
USA	North Carolina	-	Early-Middle Miocene	69.0	29.9	2.3	Wakefield, 1980
USA	North Carolina	bedded; granular	Early-Middle Miocene	62.0	26.2	2.4	Wakefield, 1980
USA	North Florida	-	Miocene-Pliocene	86.0	28.1	3.1	Wakefield, 1980
USA	Idaho	peloidal	Middle-Late Permian (late paleozoic)	135.0	32.7	4.1	Wakefield, 1980
USA	Central Florida	-	Neogene	140.0	33.3	4.2	Wakefield, 1980

USA	Central Florida	-	Neogene	140.0	33.0	4.2	Wakefield, 1980
USA	Idaho	peloidal	Middle-Late Permian (late paleozoic)	138.0	31.3	4.4	Wakefield, 1980
USA	Central Florida	-	Neogene	152.0	32.5	4.7	Wakefield, 1980
USA	Central Florida	-	Neogene	156.0	30.1	5.2	Wakefield, 1980
USA	Central Florida	-	Neogene	166.0	30.5	5.4	Wakefield, 1980
USA	Kentucky	Nodular	Upper Devonian-Lower Carboniferous	20.6	23.4	0.9	Zanin et al. 2000
USA	Kentucky	Nodular	Upper Devonian-Lower Carboniferous	53.4	23.6	2.3	Zanin et al. 2000
USA	phosphoria formation	Bedded (microcrystalline)	Upper Permian	41.7	13.0	3.2	Zanin et al. 2000
USA	phosphoria formation	Bedded (microcrystalline)	Upper Permian	108.5	33.8	3.2	Zanin et al. 2000
USA	phosphoria formation	Bedded (microcrystalline)	Upper Permian	123.1	23.2	5.3	Zanin et al. 2000
USA	phosphoria formation	Bedded (microcrystalline)	Upper Permian	194.0	34.2	5.7	Zanin et al. 2000
Venezuel a	-	Late Cretaceous-Paleogene	65-80, 72	27.9	3.5	Volkov, 1994	
Venezuel a	Recieto	-	-	51.0	15-35.6, 25.3	1.8	Van Kauwenbergh, 1997
Western Sahara	Bu Craa	Granular	Paleocene	40-90, 65	37.0	2.6	Pokryshkin, 1981
Russia	Kola	Igneous type	-	6.0			Menzel, 1968
Finland	-	Igneous type	-	0.2			Schnug et al., 1996
Russia	Kola	Igneous type	-	3.0			Schnug et al., 1996
South Africa		Igneous type	-	10.0			Schnug et al., 1996

South Africa	-	Igneous type	23.0	schnug, 2007
Brazil	Araxa	Igneous type	-	Syers et al., 1986
Brazil	-	Igneous type	117.0	
Brazil	-	Igneous type	59.2	
Brazil	-	Igneous type	18.7	this study
China	Hebei	Igneous type	-	this study
China	Hunan	Igneous type	0.3	this study
Finland	-	Igneous type	2.7	this study
Russia	Kola	Igneous type	0.9	this study
Russia	Kola	Igneous type	3.2	this study
Russia	Kola	Igneous type	3.7	this study
Russia	Kola	Igneous type	3.5	this study
Russia	Kola	Igneous type	2.5	this study
Russia	Kola	Igneous type	27.0	this study
Russia	Araxa	Igneous type	247.0	this study
Brazil	Catalao	Igneous type	220.0	Van Kauwenbergh, 1997
Finland	Silinjärvi	Igneous type	37.0	Van Kauwenbergh, 1997
Russia	Kola	Igneous type	20.0	Van Kauwenbergh, 1997
Russia	Kola	Igneous type	20.0	Van Kauwenbergh, 1997
Russia	Kola	Igneous type	30.0	Van Kauwenbergh, 1997
Russia	Phalaborwa	Igneous type	40.0	Van Kauwenbergh, 1997
South Africa	Phalaborwa	Igneous type	8.0	Van Kauwenbergh, 1997
South Africa	Phalaborwa	Igneous type	37.0	Van Kauwenbergh, 1997

Sweden	Kiiruna	Igneous type	-	20.0		
Zimbabw e	Dorowa	Igneous type	-	8.0	33.1	0.2

837 **Table S2. $\delta^{18}\text{O}_p$ in sedimentary phosphate rocks of different geological ages in**
 838 **this study.**

Country	Deposit	Age	Estimated age (Million years)	$\delta^{18}\text{O}_p$ (‰ VSMOW)
Algeria	-	Cretaceous-Eocene	58	20.9
Algeria	-	Cretaceous-Eocene	58	21.1
Algeria	-	Cretaceous-Eocene	90	21.3
Algeria	-	Cretaceous-Eocene	58	21.3
Algeria	-	Cretaceous-Eocene	58	21.4
Algeria	-	Cretaceous-Eocene	58	21.4
Algeria	-	Cretaceous-Eocene	58	21.5
Brazil	-	-	-	11.2
Brazil	-	-	-	20.6
China	Yunnan, Kunming	Early Cambrian	535	12.2
China	Hubei, Yichang	Late Proterozoic	770	12.3
China	Hubei, Jingmen	Late Proterozoic	770	12.4
China	Yunnan, Kunming	Early Cambrian	535	12.9
China	Sichuan, Hanyuan	Middle-Late Devonian	376	12.9
China	Guizhou, Kaiyang	Late Proterozoic	770	13.2
China	Yunnan, Jinning	Early Cambrian	535	13.8
China	Hunan, Shimen	Late Proterozoic	770	14.5
China	Hubei, Yichang	Late Proterozoic	770	14.7
China	Hubei, Yichang	Late Proterozoic	770	15.1
China	Hubei, Yichang	Late Proterozoic	770	16.1
China	Hubei, Jingzhou	Late Proterozoic	770	17.0
China	Sichuan, Shijiao	Middle-Late Devonian	376	17.4
China	Hubei, Jingzhou	Late Proterozoic	770	18.2
Israel	-	Late Cretaceous	83	19.0
Israel	Arad	Late Cretaceous	83	20.0
Israel	-	Late Cretaceous	83	20.0
Israel	-	Late Cretaceous	83	20.0
Israel	Arad	Late Cretaceous	83	20.1
Israel	-	Late Cretaceous	83	20.2
Israel	-	Late Cretaceous	83	20.2
Israel	Nahal Zin	Late Cretaceous	83	20.3
Israel	Oron	Late Cretaceous	83	20.9
Israel	Nahal Zin	Late Cretaceous	83	20.9
Morocco	-	Late Cretaceous	72	19.2
Morocco	-	Late Cretaceous	72	19.5
Morocco	Khouribga	Late Cretaceous-Middle Eocene	72	20.1
Morocco	-	-	-	20.1

Morocco	-	-	-	20.1
Morocco	-	-	-	20.2
Morocco	Khouribga	Late Cretaceous-Middle Eocene	72	20.5
Morocco	Khouribga	Late Cretaceous-Middle Eocene	72	20.5
Senegal	Taiba	Middle Eocene-Oligocene	34	19.7
Senegal	Taiba	Middle Eocene-Oligocene	34	20.3
Syria	Khnefies	Late Cretaceous	83	18.8
Syria	Ain Layloun	Cretaceous	105	21.7
Togo	-	-	-	19.8
Togo	-	-	-	20.0
Togo	-	-	-	20.2
Togo	-	-	-	20.4
USA	-	-	-	20.1
USA	Florida	Miocene-Pliocene	13	20.8
USA	Florida	Miocene-Pliocene	13	21.0
USA	Florida	Miocene-Pliocene	13	21.2
USA	North Florida	-	13	21.3
USA	-	-	-	21.3
USA	Florida	Miocene-Pliocene	13	21.4
USA	South Florida	-	13	21.4
USA	Florida	Miocene-Pliocene	13	21.5
USA	Florida	Miocene-Pliocene	13	21.6
USA	Florida	Miocene-Pliocene	13	21.7
USA	-	-	-	21.8
USA	North Florida	Early-Middle Miocene; Holocene	0.01	22.1

839

840 **Table S3. $\delta^{18}\text{O}_p$ in igneous phosphate rocks from different deposits in this**
 841 **study.**

842

Deposit	$\delta^{18}\text{O}_p$ (‰ VSMOW)
Brazil	8.8
Hebei, China	6.5
Hebei, China	6.8
Liaoning, China	6.8
South Africa	8.6
Kola, Russia	5.2
Kola, Russia	5.7
Kola, Russia	5.4
Kola, Russia	5.2

843

844